

Treball final de grau

Estudi: Grau en Enginyeria Biomèdica

Títol: Two-photon lithography for fabrication of implantable drug delivery devices

Document: Treball final de grau

Alumne: Judith Pons I Tarrés

Tutor: Josep Vehí

Departament: Enginyeria elèctrica, electronica I automàtica

Àrea: Enginyeria de sistemes I informàtica

Convocatòria (mes/any): Juny/2022

ACRONYMS

MVP: minimum viable product

SLA: stereolithography

SEM: scanning electron microscope

3D: 3 dimensions

DLW: direct laser writing

2PP: two-photon polymerization

1PA: one-photon absorption

2PA: two-photon absorption

UV: ultraviolet

DiLL: dip-In 3D laser lithography

NIR: near-infrared

DPP: dynamic precision printing modes

IP: iontophoresis

ITO: indium-tin-oxide

MF: medium features

PGMEA: propylene glycol methyl ether acetate

NaCl: sodium chloride

TBAC: tert-butyl acetate

PEGDA: poly (ethylene glycol) diacrylate

BOV: block overlap

LOV: layer overlap

OV: overlap

CLP: core laser power

SLP: shell laser power

LP: laser power

TABLE OF CONTENTS

1.	INTRODUCTION	1
2.	PREVIOUS CONCEPTS	2
	2.1 PRINTING TECHNIQUES	2
	2.1.1 Two-photon polymerization	2
	2.1.2 Nanoscribe	3
	2.1.3 Stereolithography	5
	2.2 DRUG DELIVERY	6
	2.2.1 Iontophoresis	6
	2.2.2 Cisplatin	8
3.	STATE OF THE ART	9
4.	HYPOTHESIS AND OBJECTIVES	11
5.	MATERIALS AND METHODS	12
	5.1 DEVICE DESIGN CONSIDERATIONS	12
	5.2 DEVICE FABRICATION	13
	5.2.1 Device design	13
	5.2.2 Printing preparation	13
	5.2.3 Printing procedure	14
	5.2.4 Post-printing procedure	16
	5.3 DEVICE TESTING	17
	5.4 MEMBRANE FABRICATION	18
	5.5 MEMBRANE TESTING	19
	5.5.1 Set up to calculate the membrane diffusion	19
6.	RESULTS	21
	6.1 DEVICE RESULTS	21
	6.2 DEVICE TESTING	27
	6.3 BASE FABRICATION	28
	6.4 PORES ADDITION	29
	6.5 MEMBRANE FABRICATION AND TESTING	30
7.	DISCUSSION	32

7.1 LIMITATIONS	33
7.2 SDG'S CONTRIBUTION	33
8. CONCLUSIONS	34
9. BIBLIOGRAPHY	36
10. APPENDIX	38
APPENDIX A. PLANIFICATION	38
APPENDIX B. CODE	40
APPENDIX C. BUDGET	41
APPENDIX D. ETHICS COMMITTEE	42
APPENDIX E. SLA PROCEDURE	43
APPENDIX F. PRINTING CONSIDERATIONS.....	44
F.1 NANOSCRIBE JOB RECIPE PARAMETERS.....	44
F.2 DEFAULT RECIPES FOR THE MF SOLUTION SET	48
F.3 PRE-PRINTING CONSIDERATIONS	49
APPENDIX G. DETAILED PRINTING PROCEDURE	52
G.1 Sample preparation.....	52
G.2 Sample loading, printing and sample unloading.....	53
G.3 Axiovision live-view camera settings	55
G.4 Post printing cleaning.....	55
APPENDIX H. MATERIALS AND MACHINES	56
H.1 Materials	56
H.2 Machines	57

TABLE OF FIGURES

FIGURE 1: 1 AND 2 PA. EXCITED-STATE IS REACHED AND TRIGGERS POLYMERIZATION OF A SUITABLE RESIN....	2
FIGURE 2: COMPARISON BETWEEN 1 AND 2 PA. (IMAGING FLUORESCENCE AND INTENSITY DISTRIBUTION)....	2
FIGURE 3: NANOSCIBE GT2 MODEL (©2007-2022 NANOSCRIBE GMBH & Co. KG)	3
FIGURE 4: CONVENTIONAL 3D DIRECT LASER WRITING LITHOGRAPHY VS. DIP-IN 3D LASER LITHOGRAPHY	4
FIGURE 5: ASIGA MACHINE AND DLP-SLA	5
FIGURE 6: ILLUSTRATION OF A TYPICAL IONTOPHORESIS SETUP FOR THE DELIVERY OF A POSITIVELY CHARGED DRUG.	6
FIGURE 7: CHEMICAL STRUCTURE OF CISPLATIN.....	8
FIGURE 8: CHEMICAL EQUILIBRIUM OF THE UNCHARGED DICHLORO-CISPLATIN AND THE POSITIVELY CHARGED MONO AQUA-CISPLATIN (POSITIVE ION $\text{Pt}(\text{NH}_3)_2\text{Cl}_2^+$).....	8
FIGURE 9: ILLUSTRATION OF LEDUC'S RABBIT EXPERIMENT. TWO RABBITS ARE ELECTRICALLY CONNECTED IN SERIES. ONE PAW OF RABBIT I IS COVERED IN STRYCHNINE SULFATE, ONE PAW OF RABBIT II IS COVERED IN POTASSIUM CYANIDE AND AN ELECTRIC CURRENT IS APPLIED	9
FIGURE 10: MALLIARAS GROUP, BOTH DEVICES: ON THE LEFT THE FIRST PROTOTYPE, ON THE RIGHT THE NEWEST..	10
FIGURE 11: PROGRESSION OF THE STRUCTURE.....	12
FIGURE 12: INVENTOR AND DESCRIBE SOFTWARES, RESPECTIVELY	13
FIGURE 13: PARAMETER SWEEP OPTIONS AND SCRIPT WITH THE RECIPE VALUES	14
FIGURE 14: SUBSTRATES AND CHEMICALS USED (ITO-COATED SUBSTRATES 3D MF DILL AND ACETONE AND ISOPROPANOL)	15
FIGURE 15: OBJECTIVE MOUNTING	15
FIGURE 16: ULTRASONIC BATH	16
FIGURE 17: FIRST SOLUTION OPTION (FIRST PICTURE REPRESENTS THE NEEDLE INSERTION WITHOUT ANY HELP)	17
FIGURE 18: BASE STRUCTURE.....	17
FIGURE 19: GLUING RESULT	18
FIGURE 20: PROCEDURE FOR THE MEMBRANE TESTING	19
FIGURE 21: FLOW SENSOR CONNECTED TO A PRESSURE CONTROLLER TO CALCULATE THE RELATIONSHIP BETWEEN Q AND P	20
FIGURE 22: PRESSURE CONTROLLER, FLOW SENSOR AND REAL SET UP TO CALCULATE THE DIFFUSION	20
FIGURE 23: PRINTED DEVICE	21
FIGURE 24: PRINTING STRUCTURE AND FIRST PRINTING VS SECOND PRINTING	22
FIGURE 25: DEVICE STRUCTURE AND RESULTS.....	22
FIGURE 26: INCREASE OF THE SURFACE AREA SUPPORT STRUCTURE AND INCREASE OF THE BLOCK OVERLAP .	23
FIGURE 27: PRINTING RESULT	23
FIGURE 28: PRINTING RESULTS	24
FIGURE 29: RESULTS AFTER TRYING DIFFERENT VALUES FOR THE BLOCK AND LAYER OVERLAP.....	25

FIGURE 30: PRINTING RESULTS	25
FIGURE 31: THE HIGHER THE HATCHING DISTANCE, THE LESS OVERLAP BETWEEN EACH VOXEL AND THE DARKER IT LOOKS	25
FIGURE 32: PRINTING RESULTS	26
FIGURE 33: PRINTING RESULTS	26
FIGURE 34: RESULTS FROM CHANGING THE SHARE ANGLE	26
FIGURE 35: DEVICES WITH REMAINING RESIN INSIDE AND DEVICES WHEN IT HAS BEEN VANISHED (SONICATION)	27
FIGURE 36: ON THE LEFT THE FIRST HELIX STRUCTURE AND ON THE RIGHT THE FINAL ONE (BIGGER ANGLES)	27
FIGURE 37: DEVICECUTD TO AVOID SPINNING FIGURE 38: DEVICE PRINTING ORIENTATION.....	28
FIGURE 39: FIRST BASE PRINTING FIGURE 40: UPPER BASE NEEDLES PATH AND FINAL UPPER BASE NEEDLE PATH	28
FIGURE 41: FINAL DEVICE.....	28
FIGURE 42: DEVICE IMAGES USING SEM USING DIFFERENT PORES SIZES.	29
FIGURE 43: REASON WHY EVEN THOUGH THE PORES WERE BIGGER THAN THE VOXEL SIZE, THE RESULTS WERE NOT THE EXPECTED	29
FIGURE 44: DIFFERENT PORES TYPES TRIED STRUCTURES	30
FIGURE 45: (2) AND (3) RESPECTIVELY.....	30
FIGURE 46: RESULTS OF THE MEMBRANE TESTING	30
FIGURE 47: FLOW RATE VS PRESSURE AND THE PYTHON SCRIPT TO GENERATE THE GRAPH.....	31
FIGURE 48: DEVICE WITH THE ELECTRODE.....	32
FIGURE 49: IMPLANTATION OF THE DEVICE IN DEAD MICE	34
FIGURE 50: DOUBLE MEMBRANE	35
FIGURE 51: PRINTING PROCESS.....	43
FIGURE 52: DEFINITION OF THE SLICING AND HATCHING DISTANCE THAT CREATES THE BUILDING BLOCKS FOR TWO-PHOTON POLYMERIZED STRUCTURES	46
FIGURE 53: PRINTED CUBOID SPLIT INTO TWO BLOCKS WITH VARIOUS STITCHING ANGLES. THE SHADOWING EFFECT AT THE STITCH INTERFACE CAN BE OBSERVED AT LOW ANGLES.....	47
FIGURE 54: LAYER AND BLOCK OV	47
FIGURE 55: COMPARISION OF RECIPE SOLUTIONS FOR THE 3D MF SOLUTION SET	48
FIGURE 56: SCRIPT GENERATED AUTOMATICALLY	49
FIGURE 57: INFORMATION ABOUT THE REQUIRED PRINTING DISTANCE BETWEEN STRUCTURES THAT EXCEED THE WORKING DISTANCE OF THE OBJECTIVE	50
FIGURE 58: PREVISUALIZATION OF THE STRUCTURES	50
FIGURE 59: SUBSTRATE FIXED ON (MULTI)-DILL SAMPLE HOLDER.....	53
FIGURE 60: ITO-COATED SIDE VS NO ITO-COATED SIDE.....	53
FIGURE 61: TRANSMISSION BUTTON	54
FIGURE 62: PROPERTIES WINDOW OF AXIOVISION	55

1. INTRODUCTION

3 out of 5 people will be diagnosed with cancer at some point during their lifetimes and around a third of them will die because of it [1]. Each cancer is different but some are deadlier because we are not able to administrate the drug effectively.

With more than 12 000 new cases each year in the UK and doubling the numbers in the States, brain tumours are a common disease that directly impacts patients' life [2]. On average, only 12% of patients survive for five or more years after being diagnosed [3] and are treated by a combination of chemotherapy, radiotherapy and, if possible, surgical resection. Chemotherapy has limitations such as the blood-brain barrier, which plays a pivotal role in protecting the central nervous system from toxic substances but also significantly reduces the amount of cancer drugs that can be delivered [3]. A bad vascularization of solid brain tumours further complicates the delivery of therapeutically relevant drug doses [4]. A multitude of technologies have been developed to overcome those limitations; binding molecules to nanoparticles or using ultrasounds to temporarily disrupt the barrier. A different approach is avoiding the barrier by delivering cancer drugs directly into tumours [3, 5, 6].

The main idea of this project is to explore microfabrication of an implantable drug delivery device, concretely direct laser writing. The device should allow to electrostatically deliver charged cancer drugs into brain tumours, technology which is called iontophoresis – basically relies on the motion of ions in electric fields. This technology avoids pressure-related problems such as drug reflux and brain oedema formation [3, 7]. Different prototypes of the device will be developed and analysed to see which one works best starting with a MVP and following a continuous improvement system. Not only the fabrication technique will differ from the current one – a PhD student is developing the same device with a different printing technic (SLA), on a higher scale (3cm height) with a different structure and components but with the same goal. Among the possible alternatives will be to replace a part of the device, the 'membrane' with flat lines, nanopores, grids, spirals, etc, or to change its shape, more rounded to better fit the tumour. It is also intended to reduce the current device to 1-2mm because the smaller, the easiest it is to implant it to animals for testing the device.

Being able to fabricate a device with such drug delivery would raise the chances for the drug to get into the tumor and, as a result, become an effective treatment. Besides this, it would not have to deal with the current limitations such as drug reflux or oedema formation since it is based on ion exchange and not in liquid injections.

Nanoscribe, a high-performance laser lithography system for rapid prototyping and wafer-scale batch production will be used for this attempt.

This project combines engineering with biology, chemistry and physical principles along with 3D printing and prototyping with CAD software. This project will take place at the Bioelectronics Lab in the Electrical Engineering Department at the University of Cambridge.

2. PREVIOUS CONCEPTS

2.1 PRINTING TECHNIQUES

2.1.1 Two-photon polymerization

Two-photon polymerization, also called direct laser writing (DLW) is a high-resolution 3D photolithography technique that relies on the local solidification of a photoresist at the focus of a laser beam to “draw” structures with feature sizes down to a 100nm.

For the two photons of near-infrared light being absorbed simultaneously, we need a sufficiently high light intensity provided by a femtosecond pulsed laser beam. The laser is focused into the resin and two-photon polymerization (2PP) triggers only in the focal spot volume (Figure 2. left), where the light intensity exceeds a polymerization threshold and the excitation is limited to the voxel around the focal point. Thus, it allows the creation of precise 3D microstructures without using a photomask. The resin is otherwise transparent to the wavelength of the photons (Figure 2, right). In contrast, one-photon absorption (1PA) with equivalent energy takes place along the trace of the beam (Figure 2, right).

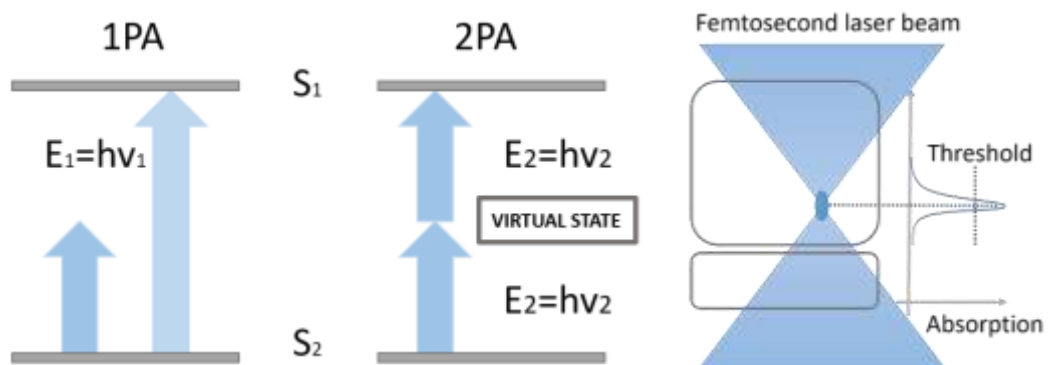


FIGURE 1: 1 AND 2 PA. EXCITED-STATE IS REACHED AND TRIGGERS POLYMERIZATION OF A SUITABLE RESIN.

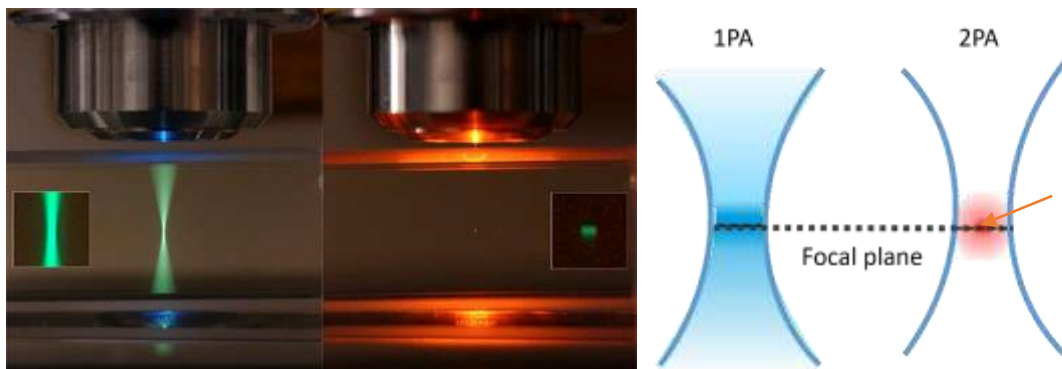


FIGURE 2: COMPARISON BETWEEN 1 AND 2 PA. (IMAGING FLUORESCENCE AND INTENSITY DISTRIBUTION). SOURCE: [HTTPS://WWW.SCIENTIFICA.UK.COM/LEARNING-ZONE/TWO-PHOTON-EXCITATION-MICROSCOPY-WHY-TWO-IS-BETTER-THAN-ONE](https://www.scientifica.uk.com/learning-zone/two-photon-excitation-microscopy-why-two-is-better-than-one)

Regarding the voxel, the smallest building block of the 3D construction known as the volume pixel, has an ellipsoidal shape and different parameters including the objective numerical aperture (NA), laser mode, and refractive index difference between the immersion system and the resist. Those determine the size and shape of the voxel and the corresponding laser focus intensity distribution.

The process takes place in the following steps: (1) Initiation, (2) Propagation and (3) Termination.

The IP-S allows chemical polymerization to occur and generate radicals as well as determines the final structure properties such as viscosity and hardness. That mainly depends on how highly photochemically active the IP-S is and allows us to maximize the potential of the 2PP process.

In terms of the photosensitive materials, the absorption of photons determines the spatial resolution of the 3D structure. Thus, we can use the same as in UV lithography for 2PP. We will particularly use negative-tone photoresists. Any form of gels, viscous liquids, or amorphous solids can be used as long as it is optically transparent to the laser wavelength. In our attempt, a negative-tone photoresist was used, particularly an acrylate-based (any IP-series resist would be suitable). As a result, laser exposure crosslinks the polymer chains, which leads to the formation of the cured 3D object on a substrate, and finally, the unpolymerized resist is removed by a solvent developer. To do that, the gel containing monomers and two-photon active photoinitiators is used as raw material. In our project, this gel, called more often resin, is IP-S which is composed of an acrylate monomer and a photon initiator (which crosslinks acrylate monomers to polymers).

2.1.2 Nanoscribe

Nanoscribe, a high-performance laser lithography system for rapid prototyping and wafer-scale batch production will be used in this project. The model used is the Nanoscribe Photonic Professional GT2 (See Figure 3).



FIGURE 3: NANOSCRIBE GT2 MODEL (©2007-2022 NANOSCRIBE GMBH & Co. KG), SOURCE: [HTTPS://WWW.NANOSCRIBE.COM/EN/PRODUCTS/PHOTONIC-PROFESSIONAL-GT2](https://www.nanoscribe.com/en/products/photonic-professional-gt2)

Nanoscribe GmbH invented a new laser lithography process called DiLL, Dip-In 3D laser lithography, to overcome the drawbacks associated with conventional direct laser writing. For instance, photoresists are not usually refractive index-matched to the oil-immersions microscopic system, thus, refractive or reflective errors resulting from this mismatch lead to intense loss of laser power and resolution as the writing depth is increased. However, in the Nanoscribe process, the objective lens is directly dipped into the liquid and an uncured photoresist acts as both a photosensitive and immersion medium in an inverted fabrication manner and the refractive index of the photoresist defines the focal intensity distribution. We are using transparent substrates (glass) but opaque substrates such as silicon can also be used. We need to be aware that transmissive substrates show better reflective illumination than the opaques ones but this last one show better adhesion. Figure 4 illustrates the difference between the conventional DLW and DiLL systems.

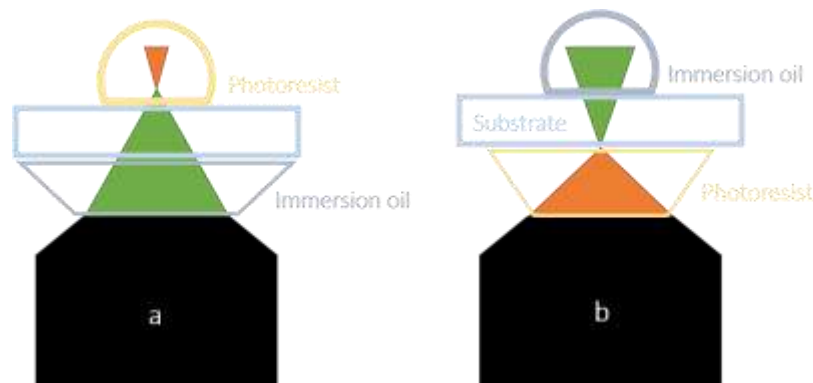


FIGURE 4: CONVENTIONAL 3D DIRECT LASER WRITING LITHOGRAPHY VS. DIP-IN 3D LASER LITHOGRAPHY

In DiLL processing (b), the objective working distance does not limit the height of the sample; therefore, structures with millimeter heights can be fabricated whereas in conventional DLW. Nanoscribe GmbH has developed a selection of commercially available 2PP-compatible proprietary IP photoresists for micro- and nanofabrication with high mechanical stability, low shrinkage, easy handling, and superior resolution. IP photoresists are negative tone and specially developed for DLW through the nonlinear absorption of femtosecond NIR laser beams in 2PP. IP-Dip, IP-S, IP-L780, and IP-Q resins are most suitable for the DiLL process. In our project we are using IP-S since it is the only biocompatible, non-cytotoxic resin - according to ISO 10993-5 /USP 87, and also because one of its possible applications is in microfluidics.

Nanoscribe has Dynamic Precision Printing modes (DPP) that are an optimization between speed and precision. All DPP modes are finely tuned starting points for quickly achieving excellent print results. With DeScribe, the print job preparation software, we customized one of the modes to fit our design and specific requirements. We used the trial and error method, so we played with the values, read lots of articles, to see recommendations, and kept trying until we achieved the results we needed.

Process recipes are a standard part of Nanoscribe products, as they enable you to create print projects in a few clicks for a broad range of applications. For specific applications, they serve as a starting point for print optimization. The five DPP modes are explained in Appendix F (F.2).

2.1.3 Stereolithography

During our device's testing we realized we needed a support that kept our device static. The base was of the order of cm and since Nanoscribe works amazingly with small structures but not with bigger ones, we chose another printing technique that allowed us to achieve better results.

Asiga, a 3D printer that builds objects from CAD data, uses stereolithography as a printing technique which is also known as SLA, particularly, DLP-SLA. (see Figure 5) a high-profile 3D printing and additive manufacturing method that uses a selective exposure to light by projector to achieve the desired product at a high manufacturing speed. These objects are built from photopolymer resins which are liquid chemicals that can be solidified by exposure to light. In our project we used GR-10 from Pro3dure, a clear biocompatible resin, but other materials such as Miicraft BV-007 can also be used. SLA consists of transforming the photosynthetic resin into solid-state layer-by-layer through single photopolymerization. The steps of the procedure are explained in more detail in Appendix E since it is not the printing technique of the device but of the support, thus is that significant for the project.

Stereolithography is an additive manufacturing process that belongs to the vat photopolymerization family but is the only one that uses UV lasers as a light source to selectively cure a polymer resin.

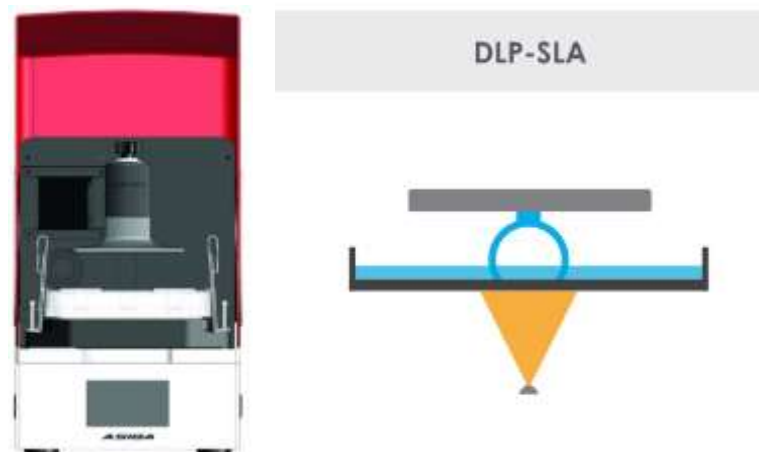


FIGURE 5: ASIGA MACHINE AND DLP-SLA. SOURCE: <https://www.whipmix.com/wp-content/uploads/2021/06/MAX-USER-GUIDE-20190916.PDF> AND <https://en.wikipedia.org/wiki/Stereolithography#/media/File:DigitalWorkflow.001.JPG>

The main difference between 2PP and SLA is that SLA scans the surface of a photosensitive material by using a UV laser to create 2D patterns of polymerized material by single-photon absorption. The fabrication is only possible layer-by-layer, whereas, in 2PP the fabrication of 3D objects is not limited to the layer-by-layer method and microstructures are created by DLW of a transparent photosensitive material which is highly absorptive in the UV range and normally transparent in the IR region.

2.2 DRUG DELIVERY

2.2.1 Iontophoresis

Iontophoresis is a method where the movements of ions across a membrane are enhanced using an externally applied potential difference, basically allows the delivery of charged molecules, and indirectly also uncharged molecules, into tissue with electric fields. Traditionally, iontophoresis was used to increase the transport of a topically applied drug formulation into the skin.

This technology avoids pressure related problems encountered with convection enhanced delivery by solely relying on the motion of ions in electric fields. The reason for the interest in iontophoresis is that this technique is very versatile allowing to deliver substances into tissue which are usually impermeable. Additionally, iontophoresis opens up the possibility to deliver drugs in a targeted fashion directly into the desired tissue instead of administering it systemically which reduces off-target toxicity. In the particular case of brain cancer, one of the hardest to treat, this technology avoids pressure related problems such as drug reflux and brain oedema formation. Much higher delivery rates are possible than when relying solely on passive diffusion of the drug. [11, 12]

Presently, known iontophoretic devices consists of, at least, two electrodes. One of the electrodes, known as the working electrode (also known as active), is placed at the position where the drug needs to be delivered, e.g. a skin tumour. To prevent tissue damage, the working electrode is usually not directly in contact with it but separated by a sponge or a piece of fabric which is soaked in a drug solution. [10] The second electrode, the counter electrode (also known as dispersive) is usually placed on a healthy patch of the patient's skin, e.g. the neck. As this electrode closes the electric circuit it also needs to be placed on an electrolyte reservoir - closes the electrical circuit that includes the first electrode, the patient's body and an energy source such as a battery. Figure 6 illustrates the setup.

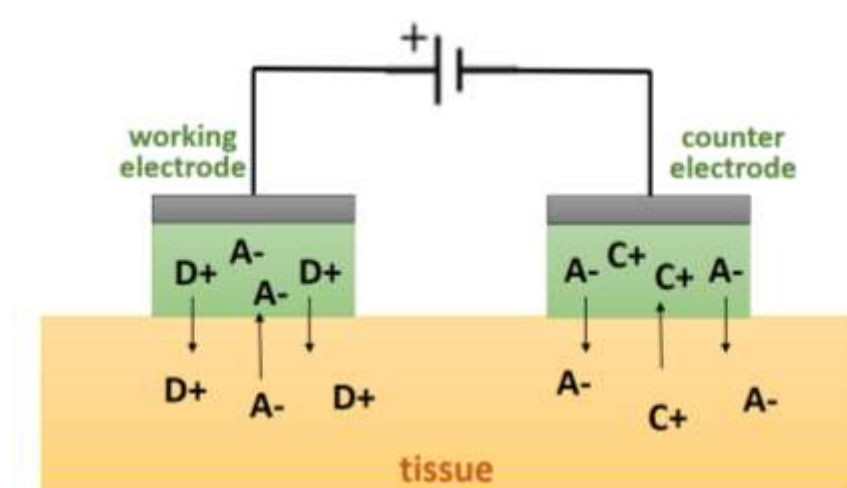


FIGURE 6: ILLUSTRATION OF A TYPICAL IONTOPHORESIS SETUP FOR THE DELIVERY OF A POSITIVELY CHARGED DRUG.

The polarity of the working electrode has the same sign as the drug molecule charge because of the way the electric source is connected to the electrodes. As a result, an electric current through the power source and an ionic current between the electrodes through the tissue sets on. The electrodes create an electric field which drives at the working electrode the drug molecules away from the electrode into the tissue. At the same time ions of the opposite charge of the drug molecules are delivered into the skin at the site of the counter electrode. The working electrode is placed on a reservoir (green area) containing the charged drug molecule D^+ and its counter ion A^- . The reservoir between the counter electrode and the skin (green area) holds an electrolyte containing both anions A^- and cations C^+ . when the current is switched on both drug molecules D^+ from the working electrode reservoir and anions A^- from the counter electrode reservoir are driven into the tissue while ions of opposite charge are attracted into the reservoirs.

We should be aware of the main factors affecting iontophoresis transport, which include compound physicochemical properties such as molecular size, charge and concentration, drug formulation, types of vehicle, buffer, pH, viscosity, presence of other ions, equipment used such as available current range, constant vs pulsed current, type of electrode, among many others. [12]

The drug transport in iontophoretic devices is dominated by the effects of diffusion and electromigration and based on electroosmosis and electrolysis. Here, I briefly introduce the main concepts:

- **Diffusion** describes the process by which molecules of matters move from high concentration towards the low concentration - is driven by concentration gradients and tries to establish a uniform concentration distribution.
- **Electromigration** describes the movement of atoms based on the flow of current through a material. If the current density is high enough, the heat dissipated within the material will repeatedly break atoms from the structure and move them. This will create both 'vacancies' and 'deposits'. It can also be described as a repulsion caused by the creation of charge imbalances in the electrolytes when a voltage is applied to the electrodes.
- **Electroosmosis** is the convective solvent flow that results from the application of an electric field across a solution next to a charged surface. It basically aids the transport of both neutral and charged species through this electric field-induced convective solvent flow. Is an effect which causes transport of bulk electrolyte through the small pores of a charged membrane when an electric field is applied. [8]
- **Electrolysis** is the passage of an electric current through a liquid containing electrically charged ions, known as electrolyte.
- **Electroporation** allows chemicals, drugs and other substances to be introduced into the cell by applying an electrical field to cells to increase the permeability of the cell membrane.

2.2.2 Cisplatin

Cisplatin ($\text{Pt}(\text{NH}_3)_2 \text{Cl}_2$) is the oldest metal-based cancer drug. Being approved for medical use in the late 1970s, it has become a well-established drug with almost half patients undergoing tumour chemotherapy in 2005 being treated with cisplatin. It has a wide range of cancer treatment forms such as sex glands, head and neck and bladder cancer. [13, 14]. Cisplatin is usually administered as an intravenous injection; the dose depends mainly of the cancer form. See figure 7 to see its chemical structure:

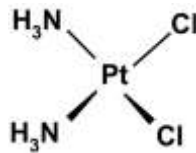


FIGURE 7: CHEMICAL STRUCTURE OF CISPLATIN, SOURCE: [HTTP://WWW.CONCONILAB.CA/PORTFOLIO/CISPLATIN/](http://www.conconilab.ca/portfolio/cisplatin/)

Since several studies in the late 1980s have shown that cisplatin is also effective for the treatment of childhood brain tumours, cisplatin has become part of the standard treatment of medulloblastomas. [15–18] Even though cisplatin has been shown to be effective in vitro against glioblastoma cells, there is no clinical evidence that cisplatin is effective when administered to glioblastoma patients. [18, 19] Moreover, NEWTON et al. report serious side-effects due to cisplatin toxicity in patients such as epileptic seizures and visual deterioration. [19] The effectiveness of cisplatin for the treatment of brain cancer is seriously limited by its toxicity and its low penetration of the blood-brain barrier. JACOBS et al. have demonstrated that the cisplatin concentration in the cerebrospinal fluid and brain extracellular fluid of rhesus monkeys is only 5 % of the concentration in the veins. [20] In a recent publication PÉREZ et al. however report that cisplatin is effective for the treatment of GL261 glioma model tumours in mice when directly injected into the tumours using convection enhanced delivery with only moderate neurological symptoms of toxicity. [18] The main idea why cisplatin was chosen it is because it is a well-established, well understood and widely used drug and brain tumour in vitro and in vivo models for cisplatin have been published. [13, 18] This eases the verification process and allows to compare the device performance to other delivery techniques such as convection enhanced delivery. [18] Additionally, cisplatin is compared to other cancer drugs such as temozolomide or gemcitabine a comparably small drug molecule. The charged molecule forms and the iontophoretic transport of cisplatin has been already demonstrated in multiple publications. [3] Monoaqua-cisplatin is a weak acid and will adjust in equilibrium to an acid pH solution (see Figure 8). Hence, commercial cisplatin formulations for cancer treatment are sold with a pH varying between 3.5 and 6.5

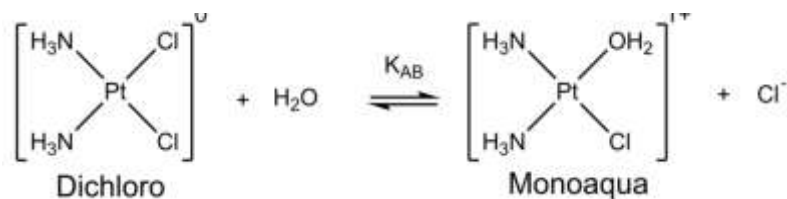


FIGURE 8: CHEMICAL EQUILIBRIUM OF THE UNCHARGED DICHLORO-CISPLATIN AND THE POSITIVELY CHARGED MONOAQUA-CISPLATIN (POSITIVE ION $\text{Pt}(\text{NH}_3)_2 \text{Cl}_2^{1+}$). SOURCE:

[HTTPS://WWW.RESEARCHGATE.NET/PUBLICATION/330323305CISPLATIN-MEMBRANEINTERACTIONSANDTHEIRINFLUENCEONPLATINUMCOMPLEXESACTIVITYANDTOXICITY](https://www.researchgate.net/publication/330323305CISPLATIN-MEMBRANEINTERACTIONSANDTHEIRINFLUENCEONPLATINUMCOMPLEXESACTIVITYANDTOXICITY)

3. STATE OF THE ART

The method of iontophoresis was first described by Pivati in 1747, however it became popular at the beginning of 20th century due to the work of Leduc who introduced the term iontotherapy (related to the administration of pharmacological agents) and formulated the laws for this process. [8] Leduc's first experiment proving the principle of iontophoresis [9, 10] consisted of using a rather rustic approach to demonstrate iontophoresis by applying strychnine sulphate onto a paw of a living rabbit and by applying potassium cyanide onto the paw of another living rabbit. Both substances are strong toxins while the strychnine ion is positively charged and the cyanide ion is negatively charged. Leduc electrically connected the other paws of the rabbits with each other, placed metal electrodes on the paws covered in poison and applied an electric current through both rabbits. In one current direction (positive pole at strychnine sulphate paw and negative pole at potassium cyanide paw) the rabbits died quickly. However, when applying the current in opposite direction both rabbits survived. [9, 10] Although this experiment might not fulfil modern day's ethical standards it vividly demonstrates how charged molecules can be electrically repulsed from an electrode into the skin when being similarly charged as the molecule. Figure 9 illustrates the experimental setup.

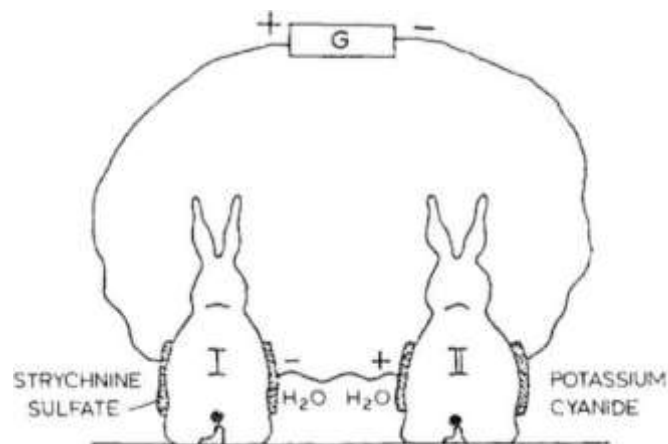


FIGURE 9: ILLUSTRATION OF LEDUC'S RABBIT EXPERIMENT. TWO RABBITS ARE ELECTRICALLY CONNECTED IN SERIES. ONE PAW OF RABBIT I IS COVERED IN STRYCHNINEGLUEIN SULFATE, ONE PAW OF RABIT II IS COVERED IN POTASSIUM CYANIDE AND AN ELECTRIC CURRENT IS APPLIED. SOURCE: [HTTPS://WWW.COSMETICSANDSKIN.COM/CDC/IONTOPHORESIS.PHP](https://www.cosmeticsandskin.com/cdc/iontophoresis.php)

Since this early experiment more than a century ago, iontophoresis is a topic of active research. So far, around 3000 publications have been published on iontophoresis. The reason for the continuing interest in iontophoresis is that this technique is very versatile allowing to deliver substances into tissue which are usually impermeable and much higher delivery rates are possible than when relying solely on passive diffusion of the drug. [14]. Additionally, iontophoresis opens up the possibility to deliver drugs in a targeted fashion directly into the desired tissue instead of administering it systemically which reduces off-target toxicity.

Currently, in Malliaras group at Cambridge University, there is an ongoing project dealing with iontophoresis as the main technique for drug delivery. The project is a continuation of Christopher M Proctor work and it is going to be published soon. Since there is a pending pattern related to it I am not allowed to give any more details. However, we will discuss Christophers work.

Since there is a huge failure in systemic drug treatments to address neurological diseases and disorders Christopher M Proctor et al. spurred the development of alternative approaches that attempt localized treatment, in 2018, they presented the utility of direct in situ electrophoretic drug delivery to treat epilepsy with precise spatiotemporal control. The unpredictability of the seizures makes the disorder particularly well suited for a therapeutic approach such as electrophoretic drug delivery which acts only when needed, for instance, just before the onset of a seizure. They used a neural probe that incorporated a microfluidic ion pump (μ FIP) which works by electrophoretically pumping ions across an ion exchange membrane to deliver only the drug of interest and not the solvent enabling precise drug release into the brain region with negligible local pressure increase. The ion pump was able to detect pathological activities and as a result stop the seizures by directly delivering neurotransmitters. Previous reports of μ FIP have shown much promise for interfacing with biology; however, challenges in scaling down these devices have limited the in vivo applications within the brain to date. [21]

Some months after, Christopher M Proctor et al., made some improvements to the previous work integrating the microfluidic ion pump (μ FIP) into a conformable electrocorticography (ECoG) device capable of electrophoretically delivering drugs and recording neural activity on the brain surface. It has been demonstrated by delivering neurotransmitters to a rodent model, that the μ FIP is able to deliver a high capacity of several biologically cationic species on demand while simultaneously recording local neural activity (see Figure 10). [22]

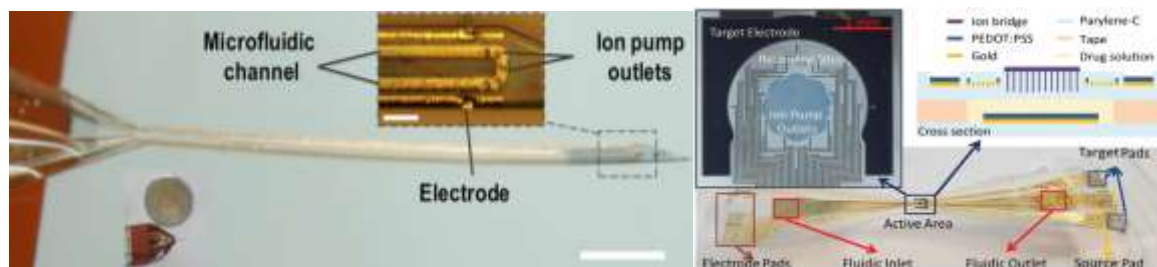


FIGURE 10: MALLIARAS GROUP, BOTH DEVICES: ON THE LEFT THE FIRST PROTOTYPE, ON THE RIGHT THE NEWEST. SOURCE: [HTTPS://WWW.SCIENCE.ORG/DOI/10.1126/SCIADV.AAU1291](https://www.science.org/doi/10.1126/sciadv.aau1291), [HTTPS://ONLINELIBRARY.WILEY.COM/DOI/10.1002/ADBI.201800270](https://onlinelibrary.wiley.com/doi/10.1002/adbi.201800270)

4. HYPOTHESIS AND OBJECTIVES

Investigation question: Does rapid prototyping allow the fabrication of sub- millimetre-sized brain implants for iontophoretic cancer drug delivery?

Hipotesis: Two-photon lithography has efficient resolution for the fabrication of micrometer size microfluidic devices which can be interfaced with macroscopic pressure controllers.

Objective: To develop a novel implantable drug delivery platform for brain cancer therapy.

To achieve the main objective, some sub-objectives need to be reached first. The specific objectives are:

- Find a way to deliver the ions before the membrane: could be nanopores, grids, flat lines, spirals, among others.
- Obtain a final device with a height around 1-2mm.
- Improve the device structure to be optimal (find the optimal value parameters and best geometry as well as the best way to place the electrode and membrane)

Additionally, we will study how to create a home made membrane for ion exchange (drug delivery) and design our own electrodes.

If this project succeeds, the devices will play an important role in addressing an efficient drug delivery while reducing off-target toxicity which is going to open the door to multiple applications to treat neurological diseases and different types of cancer.

5. MATERIALS AND METHODS

5.1 DEVICE DESIGN CONSIDERATIONS

When I was told about the project a structure with a U shape microfluidic channels was showed to me (see Figure 11; first structure). I was told that this was the main idea but that I had to think about a better way to make it, more optimal. The channels were microfluidic channels where the drug would be going through, so we needed a way for the ions to go out (ideally micropores and then a membrane to filter, I had to think about its distribution since, the more pores, the higher the drug delivery. I had to think also about the optimal shape; circle, triangle, square, heptagon, grids and spirals could be options too). To snap off the structure from the device we needed a kind of base that helped us do it easily (Figure 11; second structure). I had to think about the U shape as well. It is not the optimal one to have as much liquid as possible inside the channels. I started printing the simplest structure (U shape) and kept improving one feature at a time. Here, I briefly introduce the device printing improving progress:

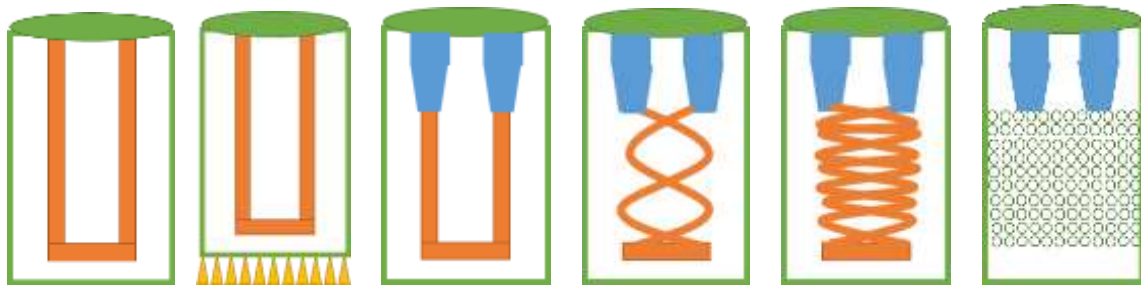


FIGURE 11: PROGRESSION OF THE STRUCTURE

After some adjustments I belived the following steps were a good start:

1. Print a device with the U shape.
2. Add a base to the device. I thought of using triangles due to a higher adhesion to the substrate and a lower on the device, making easier the snapping off of the device from the base.
3. The tub should have a conical shape so the liquid flows downwards without turbulences and the needle fits in better.
4. Make the geometry a bit more complex. I thought of doing an helix shape channel since it looks like a geometry that allows more liquid in less space, so we are increasing the total surface area.
5. Try to add the pores. I started with circles since it is one of the default forms in Inventor but it does not look like the best one since you lose a lot of space, so I will probably use another shape that allows me to create more pores using less space.
6. Add a membrane to filtre the solution but allow the pass to the drug.
7. Thinking of adding the electrode in the middle since is where we could place a straight line (between the helix and the inlet channel) but it must be a tiny electrode since the gap is not going to be precisely big.

5.2 DEVICE FABRICATION

Devices were fabricated following two-photons lithography technique using Nanoscribe GT2 model. It is recommended to take a look at Appendix G to see the real procedure, thus the information below is just a broad brushstroke of the process. The steps followed to fabricate the device were:

5.2.1 Device design

In 2PP, the desired microstructure is initially created by CAD software, in our case AutoCAD Inventor. The 3D design model from the CAD program is then converted into a Standard Tessellation Language (STL) file. The STL file is then imported into another software package (DeScribe, Nanoscribe print job preparation software; see Figure 12) for slicing into layers and parameter setup to generate the interpreted general writing language (GWL) code for printing. We tried different shapes, as well as parameters values from the job receipt until we achieved the expected result.

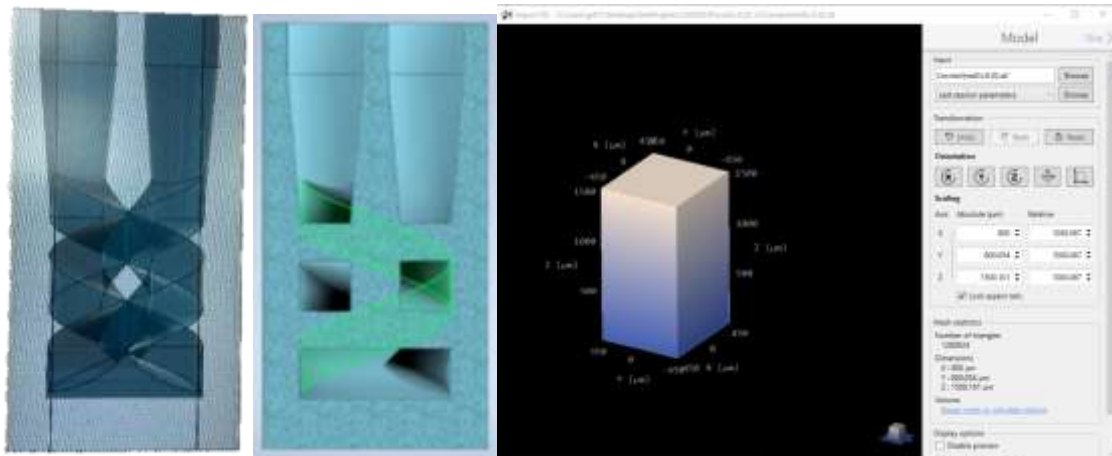


FIGURE 12: INVENTOR AND DESCRIBE SOFTWARES, RESPECTIVELY

5.2.2 Printing preparation

Before printing the device, we opened the STL file with the DeScribe, the print job preparation software of Nanoscribe. We used the *Advanced STL Processing* menu (see Figure 13) which consists of two workflows: *Batch Processing* and *Parameter Sweep*. Both are accessible through File > Advanced STL Processing. We can easily process multiple STL files using an existing recipe without stepping through the wizard using the Batch processing. But for the optimization of existing recipes (which should be done for every new structure) we changed the parameters values using Parameter Sweep (allowed us to print the same structure with different parameter values one next to the other with their labels and values printed next to the structure allowing us to compare them in a very easy and intuitive way).

In the beginning we had no idea of the optimal parameters so we used the IP-S 25x ITO Balanced swift (3D MF) receipt. IP-S refers to the resin, 25x to the objective, ITO to our substrate, MF to Medium Features (25x is always for MF and 65x for SF, S referring to small) and the one we could choose among others was the Balanced Swift which had a good precision and speed (For more information about the default recipes go to Appendix F (F.2) where they are explained in more detail). Once we found an optimal value we change the value in the recipe and load our personalised recipe (“220110_job.Recipe”) for the next printing. It was an iterative process where we kept readjusting parameters values until our device looks the way we needed. For more information about the script and the changes that need to be done see Appendix F (F.2).

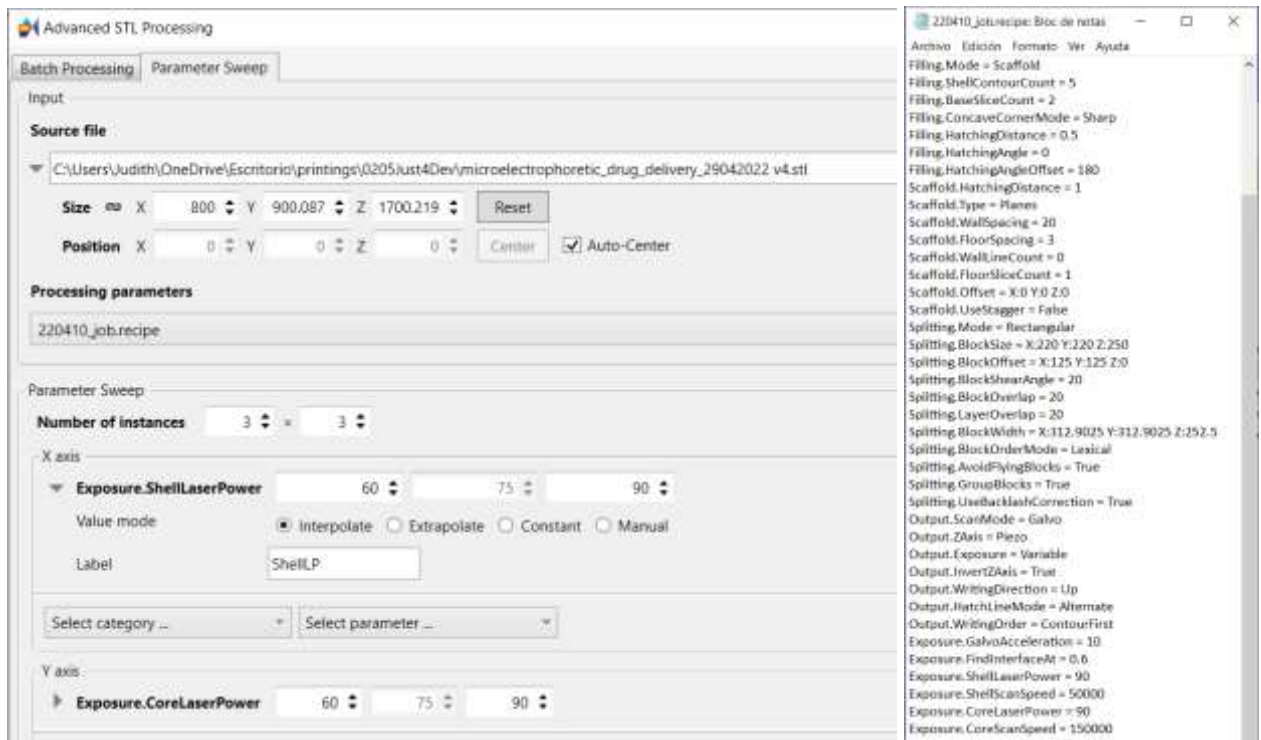


FIGURE 13: PARAMETER SWEEP OPTIONS AND SCRIPT WITH THE RECIPE VALUES

5.2.3 Printing procedure

To print a device, the following steps need to be followed: (1) Sample preparation, (2) Sample Loading, Printing and Sample Unloading, (3) AxioVision Live-View Camera Settings, (4) Sample Development, (5) Device check and test. Go to Appendix G to see the detailed printing procedure.

Regarding the sample preparation, we needed to clean the glass substrate (ITO-coated substrates 3D MF DiLL; see Figure 14) with Acetone, Isopropanol and deionized water. Afterwards, we needed to check its conductive side to apply the 2PP resin on it. This increases the refractive index contrast with respect to the 2PP resin. The ITO side can be easily identified with a multimeter. Alternative cleaning methods (e.g., oxygen plasma) have been used to deal with firstly printings when adhesion problems occurred.



FIGURE 14: SUBSTRATES AND CHEMICALS USED (ITO-COATED SUBSTRATES 3D MF DILL AND ACETONE AND ISOPROPANOL)

The substrate was fixed with sticky tape and without tilt angles in the middle of the 9 square holes' base. It was placed at the center because it offers the most uniform transmittance illumination.

Once this is done, we proceeded with the deposition of the resin which should be done in the middle and without moving the syringe too much in order not to create any bubbles.

Afterwards, the objective mounting took place. It is really important for the pupil to never contact another surface. We placed the 25x objective on the objective hole (other resolutions are for other scales or purposes) and we configured it as it is shown in Figure 15:

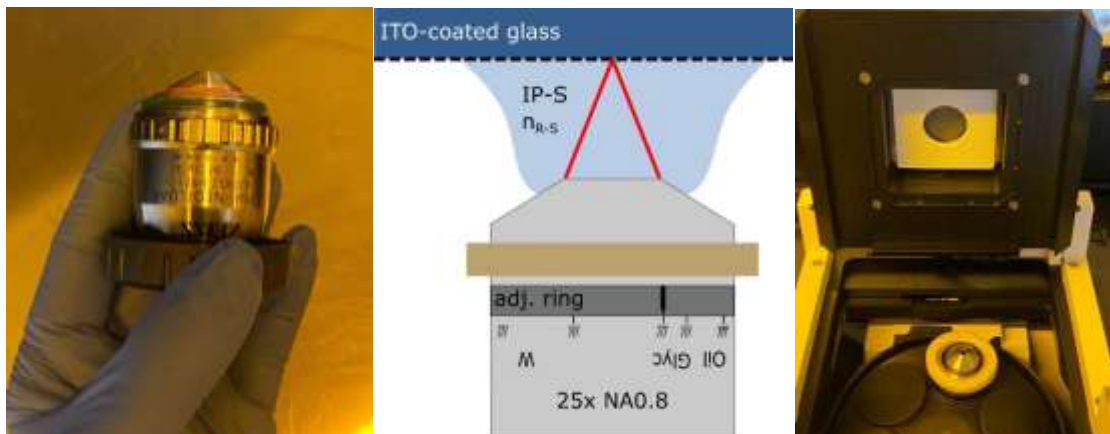


FIGURE 15: OBJECTIVE MOUNTING. SOURCE: <https://support.nanoscribe.com/hc/en-gb/articles/360002482713-25x-objective>

We also placed the felt ring to prevent 2PP resin creeping into the objective nosepiece and checked that the correct objective was selected in the microscope screen (25x).

The following step was to load the sample holder. Since we are using glass substrates we had to insert it with the label 'BOTTOM' pointing upwards (we turned it upside down in order for the objective to face with the resin). In this step is important to see 'z-lower reached' in the microscope screen and a 'choose base' window in the computer screen.

Before starting the printing, the transmission illumination button and the AxisCamera were turned on. See Appendix G (G.3) for further information.

5.2.4 Post-printing procedure

Regarding the sample development, three different methods have been used depending on the complexity of the structure. The U-shape procedure was:

- i. Remove polymerized excess of IP-S resin from the outside of the printed structure, place the entire substrate in a bath of PGMEA.
- ii. Use the substrate holder to orient the substrate vertically. Fill a 25mL beaker with PGMEA until the substrate is fully submerged into the beaker.
- iii. Leave the substrate in the beaker for 40 min (inside an air extractor, if there is no air extractor cover it to avoid evaporation of the developer)
- iv. Subsequently, lift the substrate holder out of the beaker and, with minimal delay, lower the holder into a second beaker containing isopropanol for 5min to remove the developer. (inside an air extractor, otherwise cover to avoid evaporation of the solvent).
- v. Take out the substrate and let it dry (we are not using a nitrogen pistol to blow dry because the structures are very small and would blow off)

Cleaning steps were performed in a dust-free environment illuminated with yellow light. (The procedure took place in a 10K clean room with a yellow light room). Because white light may polymerize resin sitting on top of the objective lens and make cleaning and resin removal much more difficult or even lead to permanent damage.

When we tried to inject dye through it we realized there was remaining resin that blocked the microfluidic channels. To solve it we tried two options: 1) Directly flush with the developer (PGMEA) into the microfluidic channels and 2) Use an ultrasonic bath (also known as sonication, see Figure 16). The time and power of the ultrasonic bath depends directly on the complexity of the structure geometry: the more complex, the more time and power needs to get rid of the resin. To get rid of the resin the process followed was the following:

- i. Fill a beaker (with a tap) with PGMEA (around 25ml is enough) and close the tap
- ii. Submerge sample mounted in sample holder for development in solvent
- iii. Set the ultrasonic bath temperature at 20°, power at 100% for 15min
- iv. Set the ultrasonic bath temperature at 20°, power 50% for 30min
- v. Change the PGMEA for isopropanol
- vi. Set the ultrasonic bath temperature at 20°, power 50% for 5min
- vii. It is important to clean everything properly, to know how, see Appendix G (G.4).



FIGURE 16: ULTRASONIC BATH

5.3 DEVICE TESTING

To test if the drug solution flow inside the device we inserted the syringe needles in the inlet and outlet tubes of the device. At the beginning we had lots of issues to insert the needles since the device was very small and during the insertion some devices flought away and some broke after trying to insert the needles multiple times.

On the first place we glued 30cm of Fine Bore Polythene Tubing with an inner diameter of 0.4mm and an outer diameter of 0.8mm to the syringe on one side and the needle on the other. The glue used was Norland optical adhesive 61 and cured with a curing UV light as showed in Figure 17:



FIGURE 17: FIRST SOLUTION OPTION (FIRST PICTURE REPRESENTS THE NEEDLE INSERTION WITHOUT ANY HELP)

We soon realized we needed a base to fit the device in and to be holded still when inserting the needles so they do not fall any time we touch the needles or move the device. This is where the SLA printing took place. Using Inventor, we created a base (see Figure 18) that was mainly a rectangle with a gap in the middle to hold still the device and another structure that had the support for the needles and fit perfectly with the other structure (which meant no more teezles needed nor devices lost) and that could place the needles inside the device gaps in a very easy way.

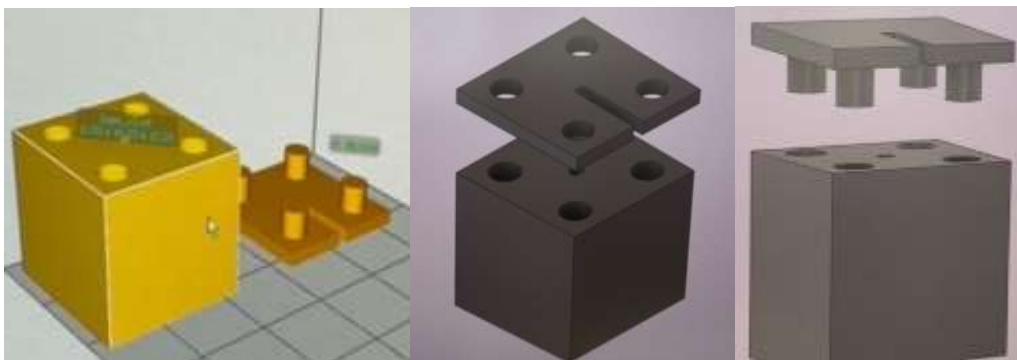


FIGURE 18: BASE STRUCTURE

Even though needles snapping off the tubes was harder, it was not impossible thus, we decided to glue the needles to the device to avoid them to snap off and prevent any kind of leakage (see Figure 19). To achieve this, we used the previous base.



FIGURE 19: GLUING RESULT

Next step was to inject dye to see if the microfluidic channels worked or if they were blocked. To do that we just inserted dye in one of the needles and see if the other one was being filled with dye.

5.4 MEMBRANE FABRICATION

Once the pores worked, we needed to create a membrane to filter the solution and just allow the cisplatin to be delivered. To do that, 3 different kind of membranes were developed:

1) Acetone and TBAC

To create the membrane we used 7.88g of Acetone in powder ($(\text{CH}_2)_2\text{CO}$), 10ml of H_2O and 3.779g of TBAC (tert-butyl acetate). We mixed the water and acetone with an orbital shaker.

ρ acetone = 0.788g/ml; molecular weight acetone = 58.08g/mol; mol weight TBAC = 277.92 g/mol

$$\text{molar concentration} = \frac{7.88\text{g/ml}}{58.08\text{g/mol}} = \frac{0.136\text{mol}}{\text{ml}} \quad (\text{Eq. 1})$$

If we add 10ml of H_2O (same as 10g because its density is $\approx 1\text{g/mL}$), we need:

$$g \text{ acetone} = \text{ml H}_2\text{O} \times \rho \text{ acetone} \left(\frac{\text{g}}{\text{ml}} \right) \quad (\text{Eq. 2}) \quad 10\text{ml} \times \frac{0.788\text{g}}{\text{ml}} = 7.88\text{g} \quad (\text{Eq. 3})$$

We used a scale to weight 10g of H_2O as well as 7.88g of acetone. We mixed both with an orbital shaker (Vortex 2). Afterwards we needed a 10% of TBAC out of the amount of acetone:

$$\frac{0.136\text{mol}}{\text{ml}} \times \frac{10}{100} = 0.0136 \text{ mol of TBAC} \quad (\text{Eq. 4}) \quad \frac{277.92\text{g}}{\text{mol}} \times 0.0136 \text{ mol} = 3.779\text{g TBAC} \quad (\text{Eq. 5})$$

We mixed everything for two hours in a magnetic hotplate stirrer.

2) Agarose and H₂O

For the second kind of membrane we just mixed 10000mg H₂O with 100mg of agarose using the orbital shaker. We let it rest for an hour until it had a similar texture to jelly.

3) H₂O, PEGDA and 2-Hydroxy-2-methylpropiophenone

The last attempt consisted of mixing 500 μ L of H₂O, 12 μ L 2-Hydroxy-2-methylpropiophenone and 0.05g PEGDA using the orbital shaker for the mixing. We let it rest also for an hour.

5.5 MEMBRANE TESTING

To test the effectivity of the membrane we first heated up the membrane to have a liquid state and dip coated the device on it and, right after, put it in cold water to cure the membrane around the device. We did it three times and then injected 20ml dye (50ml/molar methanol blue) in the needle on the inlet of the device. Afterwards, we put the device inside a UV-transparent cuvette filled with 50ml of 100m/molar NaCl and waited for 10min. To quantify the amount of “delivered” dye we used mass spectroscopy. For all the liquid measurements we used a pipette. We can see the set up in the following Figure 20:

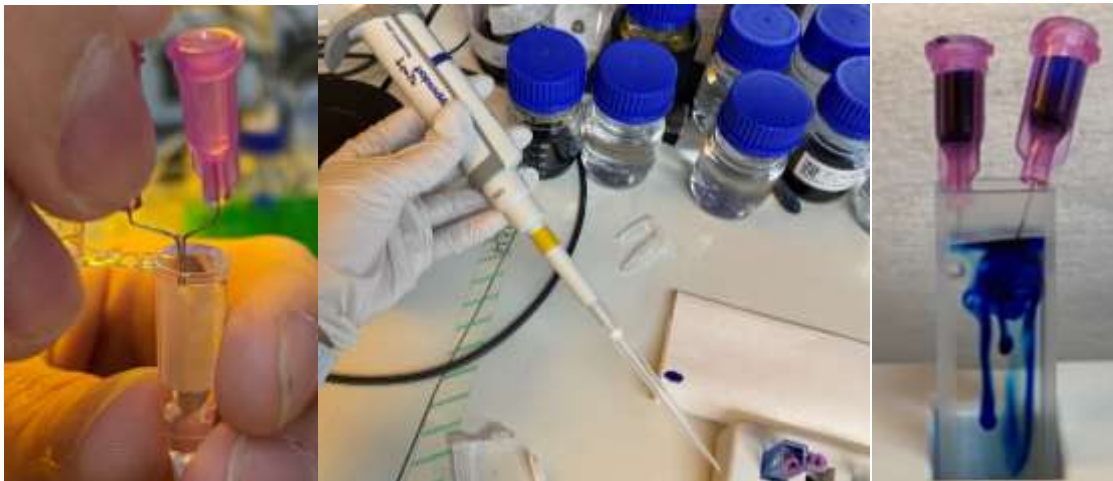


FIGURE 20: PROCEDURE FOR THE MEMBRANE TESTING

5.5.1 Set up to calculate the membrane diffusion

For the set up we used a flow sensor (FS) which gave us the flow rate: $Q(t)$. This was connected to a pressure controller (PC) which gave us the pressure: $p(t)$. We made a plot of both, $p(t)$ and $Q(t)$ depending on the time. Afterwards, we combined them to obtain a graph that plots the pressure versus the flow rate. The PC was a fluigent lineup 340mbar and the FS a sensirion 2145000155 (SLF3S-0600F). In the setup we had a beaker (reservoir full of water/dye) in which the PC applied pressure on the water and as a result it went up into the liquid system (see Figure 21 and 22 for the set up). If we think about the device (which has an inlet and an outlet) we would expect that the water goes in from the inlet and out from the outlet and pores.

If we add a membrane, we would expect this process to become harder and see a difference in the graph flow rate versus pressure. The graph also told us which pressure we needed to obtain a certain flow rate. To calculate the control, we used water in the beasel and a device without membrane. For the device (before coating and after coating) we used dye in the beasel and the computer generated a document with all the values of pressure and flowrate to plot the graphs. This was done using python.

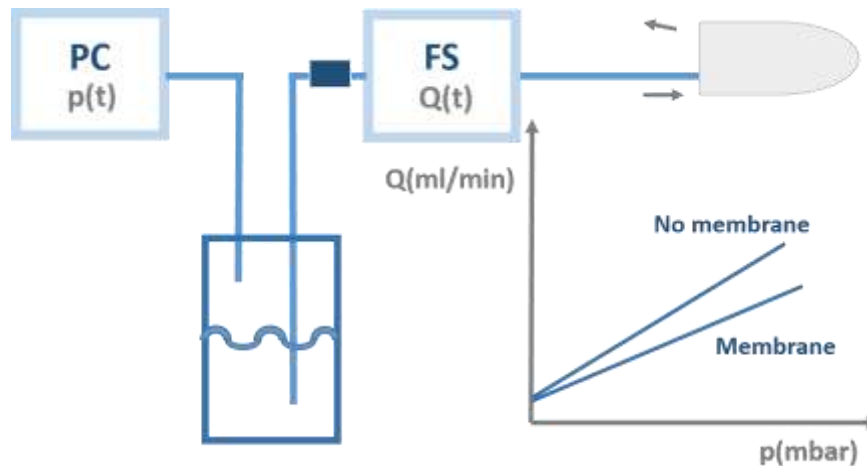


FIGURE 21: FLOW SENSOR CONNECTED TO A PRESSURE CONTROLLER TO CALCULATE THE RELATIONSHIP BETWEEN Q AND P

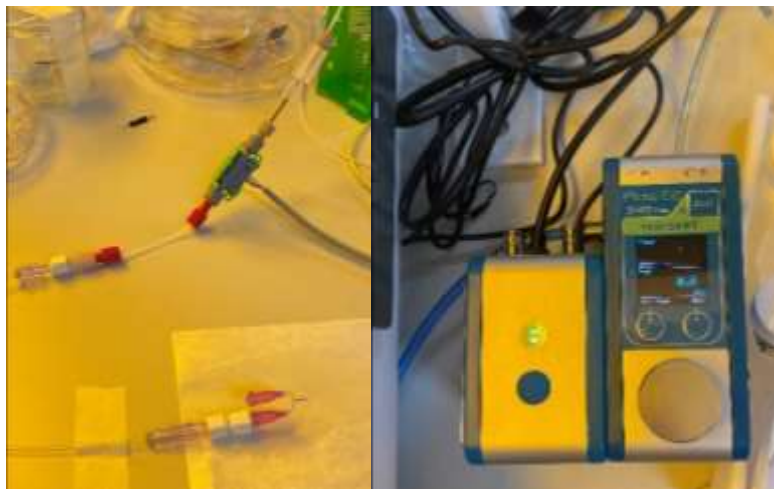


FIGURE 22: PRESSURE CONTROLLER, FLOW SENSOR AND REAL SETUP TO CALCULATE THE DIFFUSION

Regarding the regulations and legal aspects of this project, no experimentation with people of personal data were involved, thus no ethics committee had to approve nothing.

In terms of the regulations in the department, in some rooms some regulations were mandatory. In the 10K cleanroom we had to use gloves, a coat, a mask, a hairnet, overshoes and glasses. To enter the wetlab a coat, gloves and glasses were needed but for the rest of the rooms nothing was mandatory.

6. RESULTS

6.1 DEVICE RESULTS

To establish the best value parameters, we used an iteration process. On the first place, our goal was to print a decent device and keep improving its structure. Our starting point was a default recipe, the Balanced Swift 25x ITO which gave us a very first idea of the parameters values. See Appendix F (F.1) to see the default recipe and its parameter values.

1ST PRINTING: On the first printing the structure felt so we clearly had adhesion problems (see Figure 23). We observed the device on the microscope and saw that it had gaps between blocks layers. That could have been for many reasons:

1. Vignetting
2. Low block and layer overlap
3. Low hatching and sldistanceceistance
4. Low block shear angle (10°)
5. Low core and shell laser power
(higher LP, more polymerization)
6. Block sizes (too big, loses accuracy in the tips)
7. Plasma oven technique to increase the adhesion
8. Poor base (not enough surface and too tall)
9. Among many others

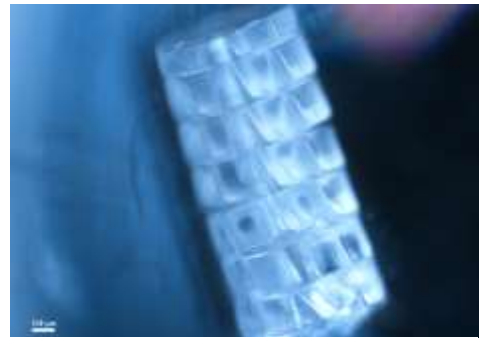


FIGURE 23: PRINTED DEVICE

After reading some literature, we realized the most significant parameters where:

- LaserPower (Shell & Core): the higher the value, the higher the polymerization.
- ScanSpeed (this last two are related so we should change one and keep the other constant).
- BlockSizes: the galvo has a resolution and the closer we get to its maximum, the less precise the printing is in that zone.
- Overlap (Block and Layer): if there is no enough OV the blocks may not stick and see gaps.
- FindInterfaceAt: where it starts drawing, very important to have a good adhesion. The recommended value is between 0.2 and 1.0.
- Shear angle: angle between blocks on the same level and hatching and slicing distance.

The parameters are better explained in Appendix F.

2ND PRINTING: The first parameter we decided to optimize was the layer and block overlap since those are the ones directly related to the gaps between blocks. The higher the value, the smaller the space between blocks. We also increased the base surface to improve adhesion (from 0.1mm to 0.2mm) and lowered the height of the device to minimize the chances of snapping off (from 2mm to 1.7mm). We printed an array of 4x4 devices with values that went from 1 to 7'5. See Figure 24.

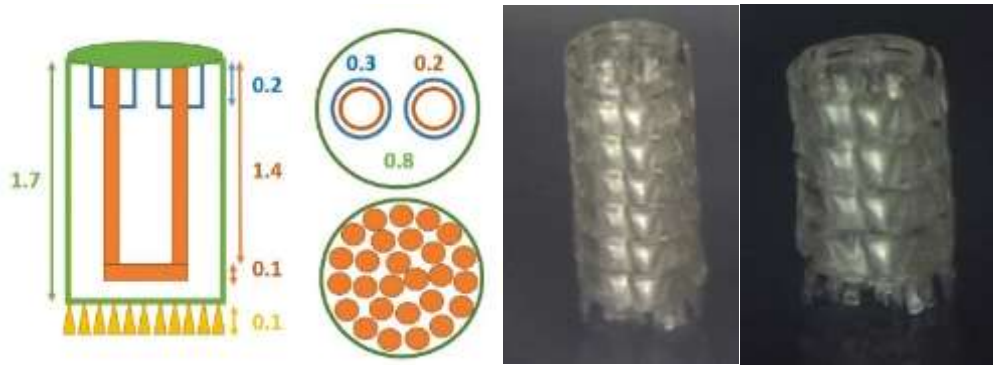


FIGURE 24: PRINTING STRUCTURE AND FIRST PRINTING VS SECOND PRINTING

RESULTS: Just 4 out of 16 structures kept in the glass, the rest fall during the post printing procedure. The 4 that remained in the substrate had a layer overlap value ≥ 6.25 . The block overlap was ≥ 2.5 so the most important related to the adhesion seems the layer overlap. The best structure was the one with the higher values. (LayerOverlap=BlockOverlap=7.5).

3RD PRINTING: Since the last printings were quite bad we decided to make a smaller device to optimise the device parameters easily. We went from a 1.8mm total length to a 0.6mm. To choose the proper Shell Laser Power and the Scaffold Laser Power (also called core) we are making a 5x5 array. The Parameters we are first changing are Shell LP on the x-axis and the Scaffold LP on the y-axis.

Just 4 out of 25 devices survived after the post-printing process (we clearly have adhesion problems) so we cannot tell which parameters are the best, but from the ones that survive the best values seem: Shell LP=40 and Core(Scaffold) LP=30. Since the structures are not good enough yet, we take out the base in the next printing so we can focus on the device structure.

ShellLaserpower	20	30	40	50	60
CoreLaserpower	20	30	40	50	60

Table 1: Values tried for shell and core laserpower

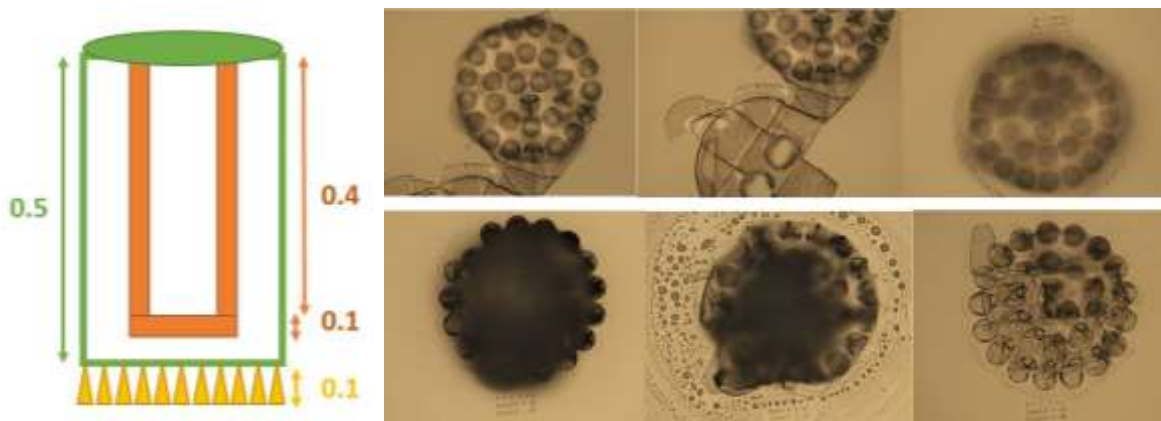


FIGURE 25: DEVICE STRUCTURE AND RESULTS

RESULTS: We can clearly observe:

- 1) Adhesion problem between the resin and the glass
- 2) Structures snap off easily (weak link between the support and the structure)
- 1) Not enough overlap (blocks do not stich well enough to each other)

The solutions could be the ones showed in the following pictures: (increasing the surface area between the support and the structure and increasing the block overlap)

We tried to take out a device from the substrate using tweezers and the device remained alright thus, we did not try to make the base since it was no longer needed.

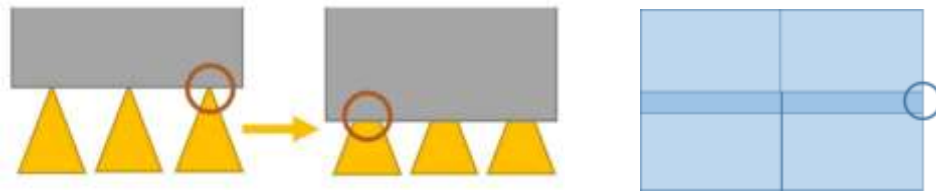


FIGURE 26: INCREASE OF THE SURFACE AREA SUPPORT-STRUCTURE AND INCREASE OF THE BLOCK OVERLAP

4TH AND 5TH PRINTING: In the following printings we tried to optimize the overlap parameters. The values we tried were, respectively (using 5x5 arrays):

BlockOverlap	2.5	3.75	5	6.25	7.5
LayerOverlap	2.5	3.75	5	6.25	7.5
BlockOverlap	5	7.5	10	12.5	15
LayerOverlap	5	7.5	10	12.5	15

Table 2: Values tried for block and layer overlap

On the first printing we realized the adhesion was not enough and playing with the parameters did not help a lot (we were not able to see the labels that indicate the values of each structure so we could not really tell which was which). However, we are using the LaserPowers we chose on the previous printing and we will play with block and layer overlap values. We were afraid that it can be because of the block size and since the galvo resolution is 350 μ m we decreased the block size from 300x300x250 μ m to 220x220x250 μ m. On the second printing we used the plasma oven to increase adhesion and see which values were the best for the overlap.

RESULT: The second printing using O₂ plasma cleaning on the substrate did not present any adhesion problems which allowed us to see that the higher values were the best for the overlap (LOV=BOV=15). On the first attempt, we realized no labels were printed on the surface. The parameter FindInterfaceAt determines the height when the printing takes place. The substrate thickness was 0.7mm and so was the value. Thus, we decided to decreased to 0.6 and, as we expected, we could see the labels on the substrate.



FIGURE 27: PRINTING RESULT

6TH AND 7TH PRINTING: Our main limitation was the adhesion so we decided to optimize the laserPower again since the higher the value, the higher the polymerization which could lead to a better adhesion. In the following printings we tried to optimize these parameters and the values we tried were, respectively:

ShellLaserPower	35	42'5	50	57'5	65
CoreLaserPower	35	42'5	50	57'5	65

ShellLaserPower	60	67'5	75	82'5	90
CoreLaserPower	60	67'5	75	82'5	90

Table 3: Values tried for shell and core laserpower

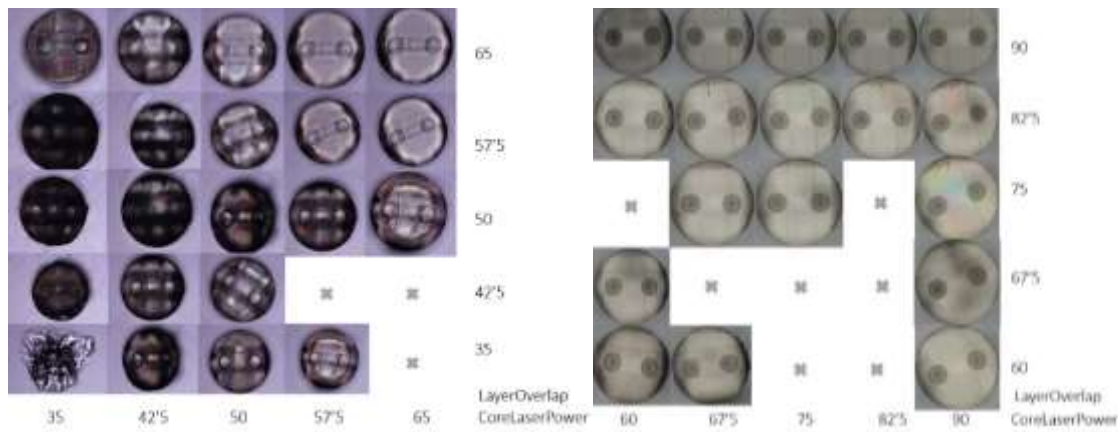


FIGURE 28: PRINTING RESULTS

RESULTS: Increasing the laserPower definitely helped with the adhesion problems (in the first printing one device fell after the post printing procedure and on the second none so it looks like the higher the laser power, the harder it is for the devices to snap off). The reason of the shadows on the corners is unknown it might be PGMEA or isopropanol that has not been dried or something else. The higher both shell and core laser power value, the better the results.

8TH AND 9TH PRINTING: So far the values we changed are: BOV=LOV=15, FindInterfaceAt=0'6, CLP=SLP=90. In this intend we tried to optimize the block and layer overlap values. Since in the last approach the highest values lead to the best results, we tried even higher values:

BlockOverlap	10	20	30	40	50
LayerOverlap	10	20	30	40	50

ShellLaserPower	10	15	20	25	30
CoreLaserPower	10	15	20	25	30

Table 4: Values tried for block and core overlap

RESULTS: As we can see in the first printing the entire 5th row was not printed that is because a BOV of 50 is too big to be even printed. If we observe the results, we might say that the LOV is more critical for stability than the BOV. If the LOV is too high and the LOV >> BOV the structures might fall as we can see in Figure 28.1, on the bottom right. For the second printing we reduced the maximum overlap values to find the optimal ones.

Any value higher than 10 and lower than 30 might be a good option so our next range of values will be between these two numbers. On the second printing, we can barely see any difference between two consecutive devices, so we just chose the medium value as the optimal.

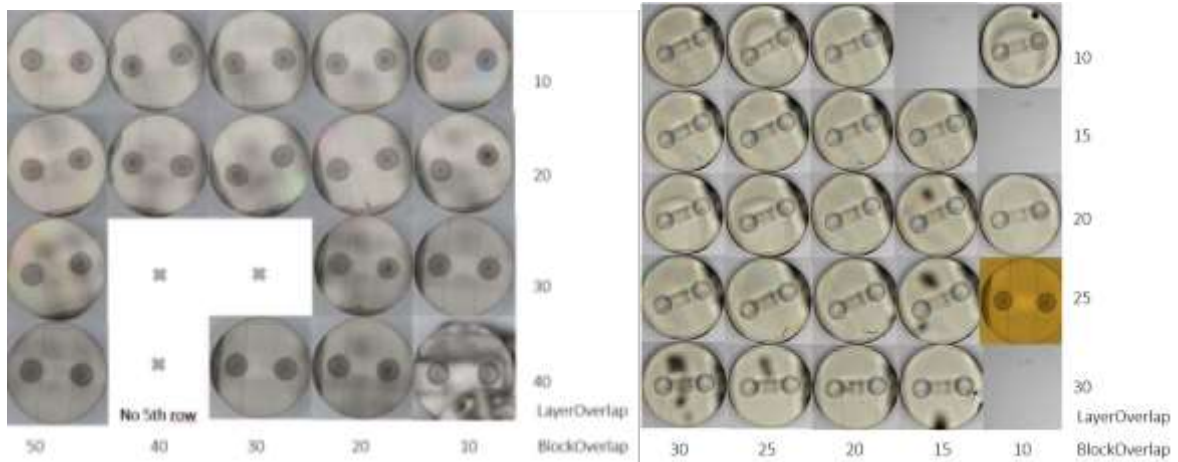


FIGURE 29: RESULTS AFTER TRYING DIFFERENT VALUES FOR THE LAYER AND BLOCK OVERLAP

10TH PRINTING: In this printing we played with two values on the x-axis (Filling.HatchingDistance; HD and Slicing.DistMax; SL) since they are both related, and one value on the y-axis (Splitting.BlockOrder; Meander and Spiral decrease time and stage movements while lexical decreases stitching error BO).

HD	0.5	0.875	1.25	1.625	2
SL	1	1.75	2.5	3.25	4
BO	Spiral	Spiral	Meander	Lexical	Lexical

Table 5: Values tried for HD, SL and BO

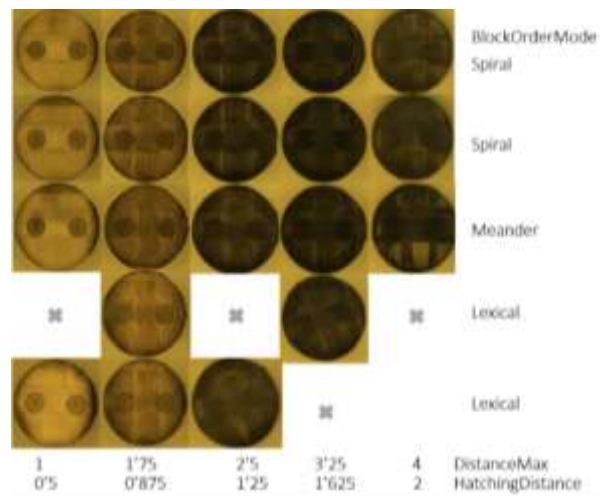


FIGURE 30: PRINTING RESULTS

RESULTS:

All block orders look alright. The best max slicing distance is 1 and the hatching distance 0.5. If we increase the hatching distance, we can see more shadows, the reason is the following one:



FIGURE 31: THE HIGHER THE HATCHING DISTANCE, THE LESS OVERLAP BETWEEN EACH VOXEL AND THE DARKER IT LOOKS

11TH AND 12TH PRINTING: Since the devices look pretty okay we are going back to the original size 1.5mm for the first printing and changing the scan speed both core and shell just to try.

RESULTS: For the first printing I just printed one device to see if there was any problem, the device looked nice and for the second one we tried higher values than the default ones to see what happened.

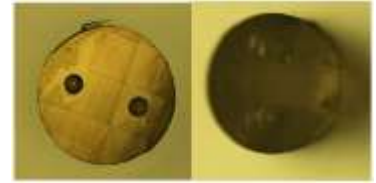


FIGURE 32: PRINTING RESULTS

Just 2 out of 9 structures were printed and one of them was very blurry and the other one tilt. Since the polymerization is already alright and we know that the laser power and the scan speed are inversely related and we do not know its precise relation continuing with this optimization would be a lost of time. It is better to leave the scan speed constant and find the optimal value changing the laser power. Doing it the other way round is also an option.

13TH AND 14TH PRINTING: We changed the splitting mode to hexagonal (instead of the rectangular, the default one). However, the printing time for the same structure was doubled so I did not start the printing and instead optimize even more the laser power and the overlap. Those are the results:

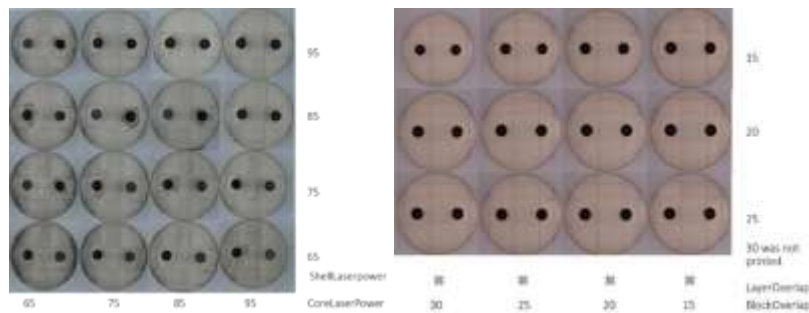


FIGURE 33: PRINTING RESULTS AFTER TRYING DIFFERENT VALUES FOR SHELL AND CORE LASERPOWER

RESULTS: We can see that the SLP and the CLP with a 95 and 85 value were the nicer but we cannot see any difference. Thus, we chose 90 the number between both. Regarding the BOV and LOV, no visible differences either so we stuck to the middle value, 20, for both.

15TH AND 16TH PRINTING: We optimized the block shear angle, the values we tried were: 15, 20, 25.

RESULTS: The three of them looked alright and very similar to the others. Thus, we just chose the middle value, 20. Since the device looked really good, the following step was to test how the dye flowed inside the microfluidic channels.

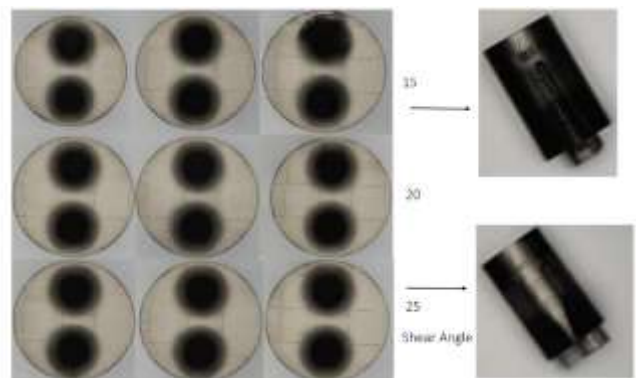


FIGURE 34: RESULTS FROM CHANGING THE SHARE ANGLE

6.2 DEVICE TESTING

When we first tried to insert the needles, we saw that it would be easier for the needle to be inserted if the channels were longer and a bit bigger (so we increased the diameter from 0.3mm to 0.35mm). This is the first thing we changed. We also finished the tube with a funnel shape for the liquid to flow downwards without turbulences and the needle to fit in better. The dye went out from the inlet which meant that the channel was not clear. Through the microscope we saw there was some resin inside the microfluidic channels that blocked them (see Figure 35).



FIGURE 35: DEVICES WITH REMAINING RESIN INSIDE AND DEVICES WHEN IT HAS BEEN VANISHED (SONICATION)

This is when the U-shape process, explained in chapter 5, took place. Afterwards, the channel was clear and the dye came out through the other channel. We realized we needed an easier way to insert the needles and test the device. We were losing devices all the time (they were very small and just flew away when we tried to insert some dye or water due to the pressure. Others just broke as a result of the tweezers pressure). As a result, a base was created (we discuss its structure and evolution in the following subchapter).

The next step was to create a more complex structure like a helix to increase the liquid volume inside the device and increase the amount of drug delivered. With the exact same procedure as the U-shape, the channels remained blocked. It makes sense since the geometry is much more complex. We decided to sonicate them for 10 more minutes and the channels were still blocked. Thus, we sonicated them for 45 more minutes and they vanished. On the next round we tried different times of sonication and none of them worked. That could have been because the helix had very small angles. We decided to make bigger ones. See Figure 36.



FIGURE 36: ON THE LEFT THE FIRST HELIX STRUCTURE AND ON THE RIGHT THE FINAL ONE (BIGGER ANGLES)

On the next round we found the helix shape procedure (basically trying different sonicating times) to unblock the channel. The structure on the left allowed the dye to flow through the device while the one on the left did not due to the unremovable resin. However, the needles did not stick inside the device so we reduced the diameter from 0,35mm to 0,3mm. The testing process with the base allows us to keep the needles inside the channels without the need to hold them.

6.3 BASE FABRICATION

The first idea was to build a cube with a hole in the middle to fit in the device. We soon realized the base needed a tope, otherwise it would be spinning around when trying to insert the needles. To solve that, we redesigned the device cutting a face and did the same for the base. See Figure 37 and 38. We also made the base a bit bigger to guarantee a good fit, e.g., the device diameter was 0.9 so the diameter of the base hole 0.95.



FIGURE 37: DEVICE CUTTED TO AVOID SPINNING

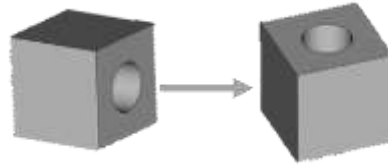


FIGURE 38: DEVICE PRINTING ORIENTATION

Once the first base was printed, we saw that the hole was not flat, it had some uniformities (See Figure 39). We printed the device as we can see in Figure 36. Since SLA is a printing process done layer-by-layer we thought changing the orientation as seen on the right of Figure 38 might solve the problem. The 4 holes added on the base were for registering the pins on the needle holder since it made the aligning and bonding of the fluidics easier. Moreover, making holes with a DLP printer like Asiga can create a vacuum that causes the print to fail. The more holes we do, the fewer the chances to create a vacuum. Afterwards, we created an upper base (needle holder) that fitted with the base and helped us insert the needles. We first designed two needles gaps and add a path until the final position (See Figure 41 in the middle). The paths were not very stable so we decided to make an improvement by cutting the material in between and keeping just the gaps that were closer to the final needle position. (see Figure 40 on the right side).



FIGURE 39: FIRST BASE PRINTING

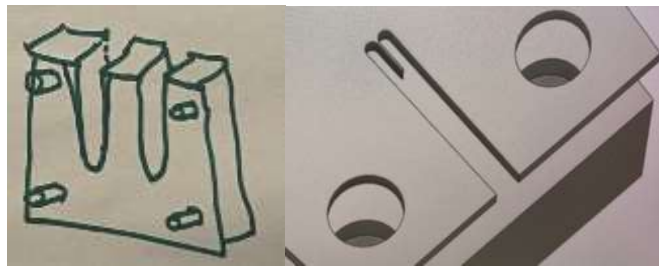


FIGURE 40: UPPER BASE NEEDLES PATH AND FINAL UPPER BASE NEEDLE PATH



FIGURE 41: FINAL DEVICE

6.4 PORES ADDITION

The next step was to create the pores around the device in the helix shape zone. Our starting diameter was 0.0015mm; 1.5 μm ; 1500nm. Since the voxel size of Nanoscribe is $\approx 300\text{nm} \times 300\text{nm} \times 1000\text{nm}$ we should be able to see this size pores. That was not the case. We were not able to see anything with the microscope so we first used the Ermetech Sputterer to dip coat gold on the device surface and turn it conductive (it is a requirement to see the image using SEM). This allowed us to obtain really high resolution images, which allowed us to see the pores shape and compare different pores sizes (see Figure 42).

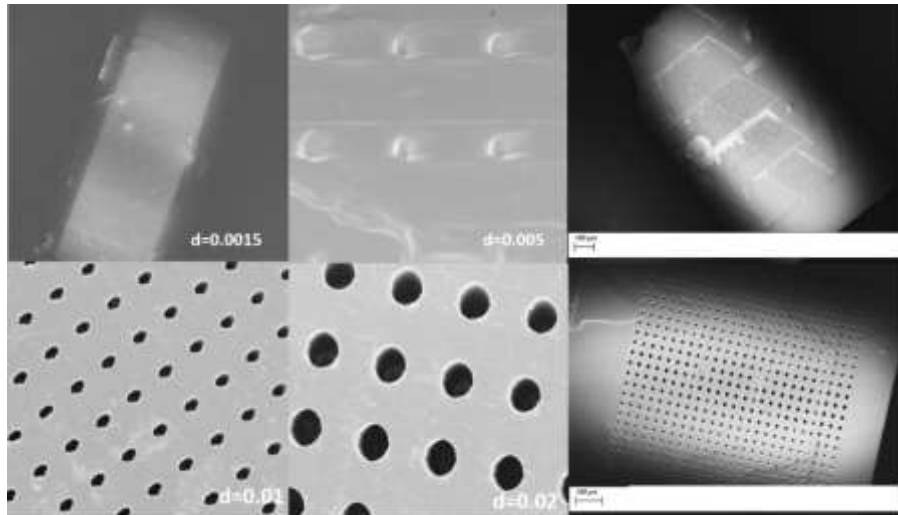


FIGURE 42: DEVICE IMAGES USING SEM USING DIFFERENT PORES SIZES.

In the first printing, we tried a diameter pore size of 0.0015mm but we could not see anything, not in the microscope, nor using SEM so we tried a higher value of 0.005mm. As we can see in Figure 43, a kind of circle was drawn but no hole made. Since it is not big enough, we tried a 0.01mm value. We were able to see the pores holes but the shape was not exactly rounded (see Figure 43). However, we tried to see if the dye flow through the pores but it all came out from the outlet. Thus, we decided to increase the diameter even more, to 0.02. We achieved a rounded shape and we were able to see dye going through the pores so we stuck with that pore size.

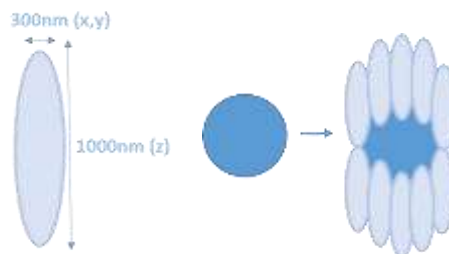


FIGURE 43: REASON WHY EVEN THE PORES WERE BIGGER THAN THE VOXEL SIZE, EVEN THOUGH THE RESULTS WERE NOT THE EXPECTED

If the diameter is very small, there might not be enough voxels to create a visible shape or the shape might be oval instead of rounded. That is because the shape size might not be big enough compared to the voxel size to create a circular shape instead of an oval shape.

We tried all kind of shapes with the goal of having as many pores as possible. The triangles seemed a really interesting shape since it allowed us to optimize the space between structures but we needed bigger “diameters” to see the proper shape. With the grid shape, some of the squares were not holded to the structure so we forgot about that option. We tried other pores shapes such as squares and hexagons but ended up sticking to circles since we knew their optimal pore size.

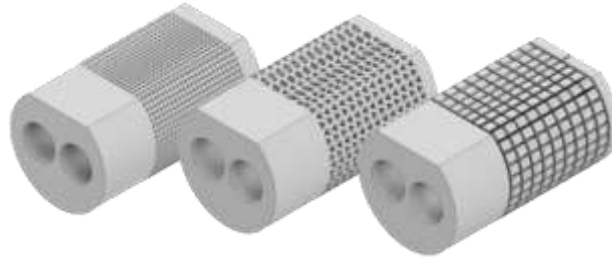


FIGURE 44: DIFFERENT PORES TYPES TRIED STRUCTURES

6.5 MEMBRANE FABRICATION AND TESTING

Just 1 out of the 3 membranes created ended up being what we expected.

- 1) **Acetone and TBAC:** We realized we ordered a different acetone than the one in the recipe. Thus, the result was a dense liquid.
- 2) **Agarose and H₂O:** We achieved a jelly texture so it looks like this one worked. (See Figure 45)
- 3) **H₂O, PEGDA and 2-Hydroxy -2-methylpropiophenone:** Just the bottom of the mix was dense the rest was liquid so it did not work.

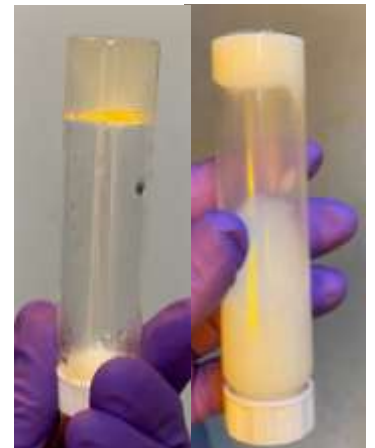


FIGURE 45: (2) AND (3) RESPECTIVELY

The results of the membrane testing procedure, described in Chapter 5, can be seen in Figure 46. We can see that there is a different concentration of dye with and without the membrane.

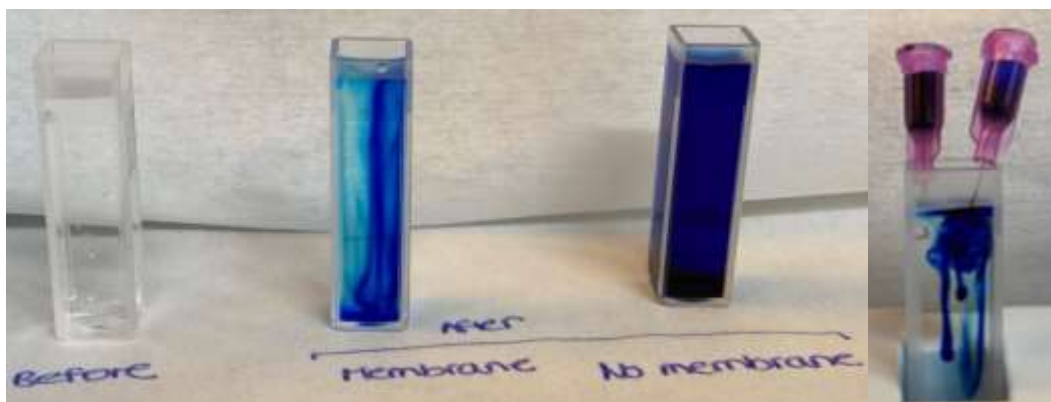


FIGURE 46: RESULTS OF THE MEMBRANE TESTING

The previous results confirm that there is an effect on the delivered dye after coating. Next step would be trying to do it with a real cisplatin solution and using mass spectroscopy to calculate the concentration of delivered cisplatin.

6.5.1 Membrane diffusion

In Figure 47 we can see the control (device in openend), the device (refers to the device before coating, so without membrane) and the device after coating (with a membrane). We can also see the y-axis error (flow rate error) which has a value of 5%. It is big enough to plot in the graph whereas the x error (pressure error) is 0.1mbar, which is too small to be plotted (See Figure 47). We see a slightly difference between the device and the device after coating. Since some values overlap if we take the error into account, the difference might be just a mere error. Thus, more precise measurements should be done to verify this.

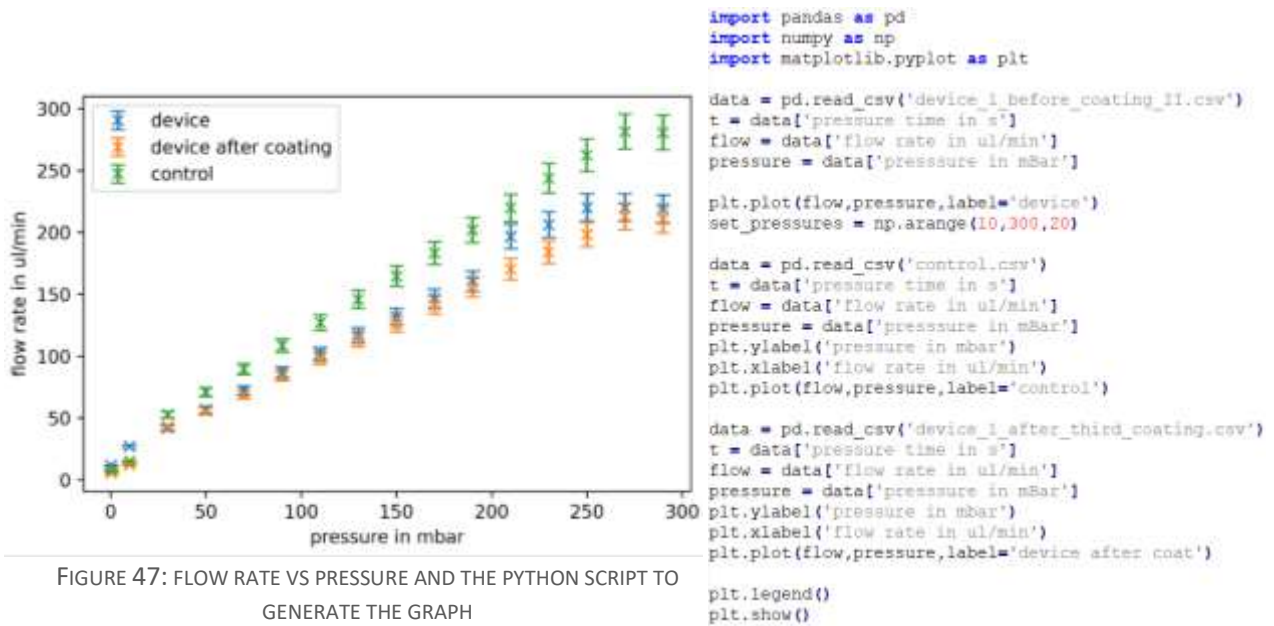


FIGURE 47: FLOW RATE VS PRESSURE AND THE PYTHON SCRIPT TO GENERATE THE GRAPH

The FS flow resistor is a PEEK tubing which is a micrometers thick tube that increases the flow resistance of the entire system. The flow of the device is very small and the PC cannot apply small enough pressure to not saturate the flow sensor. As a result, we have to increase the flow resistance of the system to move the pressure into the range of the PC. However, this can affect the results since its resistance might be much bigger than the membrane resistance. Further testing is needed to be sure about the affect over it.

In general, a thicker membrane would help us get to a conclusion since we are not sure if the dye pushed away the membrane or if the membrane is not even strong enough to stand.

7. DISCUSSION

We can confirm that rapid prototyping allows the fabrication of sub-millimetre-sized brain implants for iontophoretic cancer drug delivery and also that two-photon lithography has efficient resolution for the fabrication of micrometer size microfluidic devices which can be interfaced with macroscopic pressure controllers. Thus, we were able to achieve the main objective of the project which was the development of a novel implantable drug delivery platform for brain cancer therapy.

Regarding the sub-objectives, we found a way to create a membrane consisting of pores dip coated into a homemade membrane to filter the drug. We could not quantify the amount of cisplatin that would have been delivered from the solution since the mass spectroscopy machine broke one week before the set up and the new one was expected to arrive at ends of June. However, we were able to see that there was a difference between the amount of dye delivered before and after the coating. This is a nice attempt, however further work needs to be done. If we had more time and the mass spectroscopy machine, accurate improvements could be done.

In terms of the second sub-objective, we were able to print a device of 1.5mm height which is in between the goal range. Smaller devices were also printed but there was no point in making such small devices because the liquid volume inside the device would be too low. Finally, for the last sub-objective we did find the optimal parameters values to print the desired structure. We also improved the simple structure for a helix shape that allowed us to have more surface area to increase the volume inside the device. However, related to the electrode, we did not place it inside because we were not able to measure the drug delivery nor the electrode effect on the drug delivery. But using Inventor we can see how the device would look like (see Figure 48). The electrode was placed in the middle since it was the best way to take profit of the empty space in the middle.

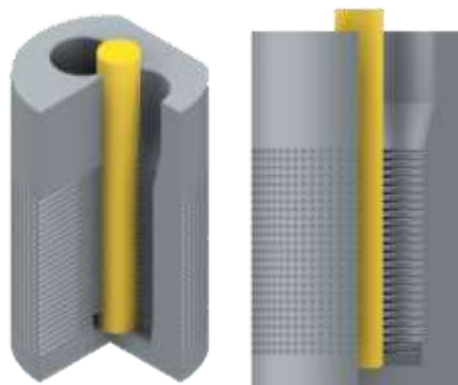


FIGURE 48: DEVICE WITH THE ELECTRODE

Regarding the additional things, we wanted to do a homemade membrane, this was accomplished while the design of the electrodes was not for lack of time. However, a simple gold string or a pencil lead are conductive materials, thus both could work as an electrode. The pencil lead is the cheapest and fastest option (there was no point in spending time and money buying materials and fabricating an electrode). Finally, we were able to see how glioblastoma was induced to mice and also we implanted the device in dead mice.

7.1 LIMITATIONS

In terms of the main and sub-objectives, the only limitation was the mass spectroscopy machine. With this machine, we could measure the drug delivery and know how good a membrane was respecting the ion exchange. Depending on the obtained results we could dip coat the device more times, see which pore shape and size worked better and know which membrane was the best, among others. If we had more time, we would also try new types of membranes and maybe compare them with some commercial ones. We did very first diffusion studies for the membrane. Further work should have been done to reach a successful conclusion. In terms of the creation of our own electrodes, is something I would have loved to do too but, because of the time left, it was not worth using it for this.

7.2 SDG'S CONTRIBUTION

Regarding the SDG (sustainable development goals; ODS in Spanish) contribution, our project contributes to the 3rd and 9th ODS. The 3rd deals with health and well-being and our project goal is to effectively administrate drugs into cancer tumors to overcome current limitations. The 9th deals with industry, innovation and infrastructures. Our project is based in innovation since we want to explore a new microfabrication technique and use iontophoresis for drug delivery, both to achieve results that have not been achieved so far.

8. CONCLUSIONS

This project was undertaken to design a novel implantable drug delivery platform for iontophoretic brain cancer therapy. The experimental section was based on the design of a micrometersize microfluidic device that fulfills the proposed objectives and its implementation and testing. The printings confirmed that two-photon lithography has efficient resolution for the fabrication of micrometersize microfluidic devices.

Overall, this study strengthens the idea that very precise microdevices can be fabricated using Nanoscribe while meeting the biocompatibility criteria, which opens the door to future applications in other areas such as neurological diseases and other cancer treatments.

Our starting point was a very basic structure; the MVP was a device with U-shape microfluidic channels. Once it fulfilled our requirements, we improved each feature, one at a time, until we achieved the final prototype: a device with helix-shape microfluidic channels, pores, membrane and room for an electrode to be placed in the middle. This methodology helped us solve the problems faster. Thus, it proved worth using a continuous improvement method instead of trying multiple things at once.

Additionally, although we did not place the electrode physically in the device, we used Inventor to see what it would look like (see Chapter 7, Figure 48). Moreover, implanting the device in dead mice (see Figure 49) allowed us to realize how small the devices were, which opened a window of possibilities regarding the use of small devices for different medical approaches. Besides, I had the opportunity to see how tumours were induced to mice and see the process that takes place in in vivo testing.



FIGURE 49: IMPLANTATION OF THE DEVICE IN DEAD MICE

A publication of this work, with me as the main autor, will take place in mid-September. The publication is going to be send to ScienceAdvances journal. On top of that, I might have the opportunity to continue with this project next course since, Jorge Malliaras, the Prince Philip Professor of Technology at the Univeristy of Cambridge was really happy about the achieved results and wanted someone to keep up with the project. Thus, some of the improvements I would do are:

- Create a more elaborate membrane (see Figure 50), the grey lines.
- Have 2 inlets and 2 oulets with helix channels to deliver drug faster.
- Make more pores in the upper part of the device and in the base.
- Try more diffusion studies in membrane coating of the device.
- Optimize the helix shape to make as many spirals as possible without compromising the flow.
- Calculate the amount of cisplatin delivered using mass spectroscopy instead of using dye.
- Place a real electrode in the device and test it.
- More studies to calculate convection and diffusion.

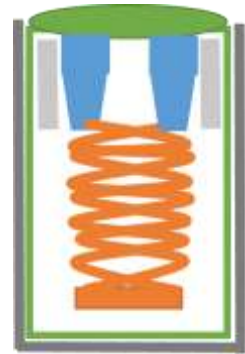


FIGURE 50: DOUBLE
MEMBRANE

Individually, any of these could be done in a short period of time but to successfully achieve all of them, around 3 months would be needed.

9. BIBLIOGRAPHY

- [1] Cancer National Institute, NIH. *Cancer statistics*. URL: <https://www.cancer.gov/about-cancer/understanding/statistics> (visited on 21/04/2022).
- [2] Cancer Research UK. *Brain, other CNS and intracranial tumours statistics*. URL: <https://www.cancerresearchuk.org/health-professional/cancer-statistics/statistics-by-cancer-type/brain-other-cns-and-intracranial-tumours> (visited on 22/04/2022).
- [3] D. S. Hersh et al. 'Evolving Drug Delivery Strategies to Overcome the Blood-Brain Barrier'. In: *Current Pharmaceutical Design* 22.9 (2016), pp. 1177–1193.
- [4] J. D. Byrne et al. 'Local iontophoretic administration of cytotoxic therapies to solid tumors'. In: *Science Translational Medicine* 7.273 (Feb. 2015), 273ra14–273ra14.
- [5] M. I. Alam et al. 'Strategy for effective brain drug delivery'. In: *European Journal of Pharmaceutical Sciences* 40.5 (Aug. 2010), pp. 385–403.
- [6] K. F. Timbie, B. P. Mead and R. J. Price. 'Drug and gene delivery across the blood-brain barrier with focused ultrasound'. In: *Journal of Controlled Release* 219 (Dec. 2015), pp. 61–75.
- [7] M. A. Vogelbaum and M. K. Aghi. 'Convection-enhanced delivery for the treatment of glioblastoma'. In: *Neuro-Oncology* 17. suppl 2 (Mar. 2015), pp. ii3–ii8.
- [8] Rawat, S., Vengurlekar, S., Rakesh, B., Jain, S., & Srikarti, G. (2008). 'Transdermal delivery by iontophoresis'. In: *Indian journal of pharmaceutical sciences*, 70. (Feb. 2008), pp. 5–10.
- [9] G. A. Fischer. 'Iontophoretic drug delivery using the IOMED Phoresor system'. In: *Expert Opinion on Drug Delivery* 2.2 (Mar. 2005), pp. 391–403
- [10] P. Tyle. 'Iontophoretic Devices for Drug Delivery'. In: *Pharmaceutical Research* 03.6 (1986), pp. 318–326.
- [11] J. D. Byrne, J. J. Yeh and J. M. DeSimone. 'Use of iontophoresis for the treatment of cancer'. In: *Journal of Controlled Release* 284 (Aug. 2018), pp. 144–151.
- [12] Y. N. Kalia et al. 'Iontophoretic drug delivery'. In: *Advanced Drug Delivery Reviews* 56.5 (Mar. 2004), pp. 619–658.
- [13] S. Ghosh. 'Cisplatin: The first metal based anticancer drug'. In: *Bioorganic Chemistry* 88 (July 2019), p. 102925.
- [14] Pfizer Labs. Cisplatin Injection. 2012.
- [15] S. J. Bertolone et al. 'A phase II study of cisplatin therapy in recurrent childhood brain tumors'. In: *Journal of Neuro-Oncology* 7.1 (May 1989), pp. 5–11.

- [16] A. B. Khan et al. 'Cisplatin Therapy in Recurrent Childhood Brain Tumors'. In: *Cancer Treatment Reports* 66 (12 1982).
- [17] R. W. Walker and J. C. Allen. 'Cisplatin in the treatment of recurrent childhood primary brain tumors.' In: *Journal of Clinical Oncology* 6.1 (Jan. 1988), pp. 62–66.
- [18] J. E. Pérez et al. 'The effect of locally delivered cisplatin is dependent on an intact immune function in an experimental glioma model'. In: *Scientific Reports* 9.1 (Apr. 2019).
- [19] H. B. Newton et al. 'Intra-arterial cisplatin for the treatment of malignant gliomas'. In: *Journal of Neuro-Oncology* 7.1 (May 1989), pp. 39–45.
- [20] S. Jacobs et al. 'Extracellular fluid concentrations of cisplatin, carboplatin, and oxaliplatin in brain, muscle, and blood measured using microdialysis in nonhuman primates'. In: *Cancer Chemotherapy and Pharmacology* 65.5 (Aug. 2009), pp. 817–824.
- [21] Proctor, C. M.; Slezia, A.; Ghestem A.; Pappa A.; Williamson, A.; Del agua I.; Malliaras, G. G. 'Electrophoretic drug delivery for seizure control'. In: *Science Advances* 4.8 (Aug. 2018), pp.1-2.
- [22] Proctor, C. M.; Uguz, I.; Slezia, A.; Curto, V.; Inal, S.; Williamson, A.; Malliaras, G. G. 'An Electroencephalography device with an integrated microfluidic ion pump for simultaneous neural recording and electrophoretic drug delivery in vivo'. In *Vivo. Adv. Biosyst* 3 (Nov. 2018), pp. 1-2.

10. APPENDIX

APPENDIX A. PLANIFICATION

During my first week in Cambridge I did a brief timeline planification for my project. It was divided by 5 months and each of them by 4 weeks (starting on Monday and finishing on Sunday instead of using particular dates). The plan was the following:

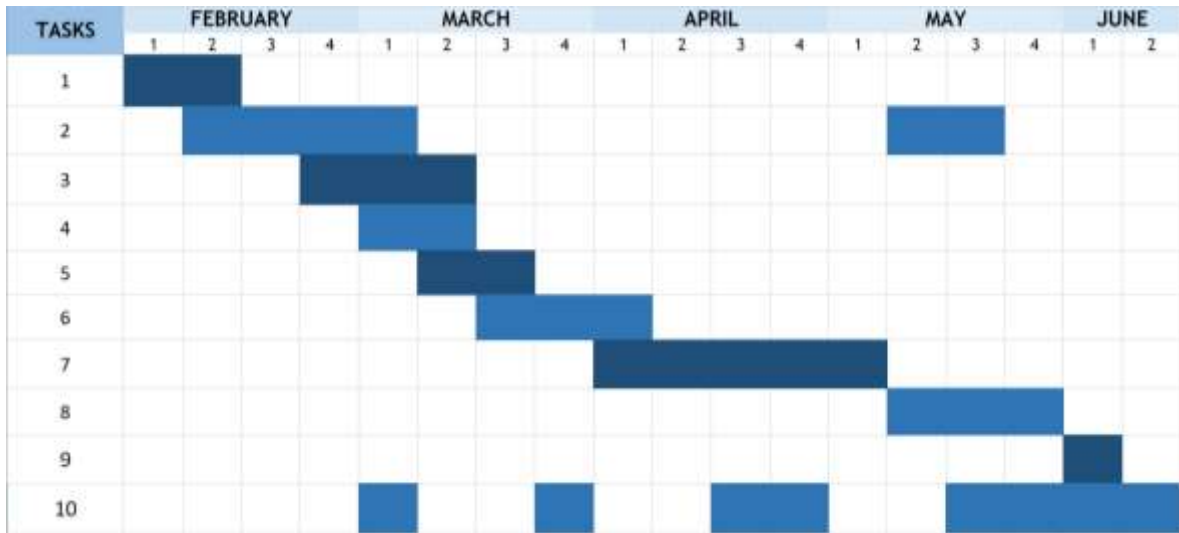


Table 6: Gantt chart

The tasks, described in more detail were:

- 1) **Inductions:** I needed to do some inductions before being able to use some rooms and machines.
- 2) **Papers:** I asked my supervisor and he told me I would be reading papers for around one month until I had an idea of everything involved in the project. He would be discussing every paper after I read it to help me consolidate the main ideas. I thought it would be a good idea to read again the most important ones after a couple months to refresh ideas.
- 3) **Nanoscribe induction:** Nanoscribe is a very delicate machine and there are different softwares you need to use to print a structure. So knowing how to use it properly is very important. I was supposed to see some printings first, then read how it is done (nanoscribe training and respective quizzes to prove the acquired knowledge) and then see some more printings again. I estimated that it would take 3 weeks to do all that.
- 4) **Learn how to use Autocad:** I never used CAD or prototyping so it was new for me. I did not know how long it was going to take so I asked my supervisor and he told me that in two weeks I would be more than familiarized with the software.
- 5) **1st supervised printings:** I was supposed to start printing by myself (first under the supervision of Tobias, the PhD student that helped me in my project and once he was sure I knew how to do it I could print by myself). I estimated 2 weeks for that being aware that it might be too much.

- 6) **Device parameters optimization:** I estimated that finding the optimal parameters would take around 3 weeks. My supervisor told me there were lots of them but around 5 that were the most important ones. If I printed arrays of 9-15 devices, it could take me around 15-20 hours to print them. So if I printed 7 days a week once a day I could do 21 different printings and repeat some parameters if needed.
- 7) **Device testing and geometry improvement:** Test if the device accomplished the requirements and afterwards improve the geometry. I overestimated the time because I might have some issues so I rather find out I needed less time than the other way round.
- 8) **Adding the pores, membrane and electrodes to the device:** Different pores sizes and shapes as well as membrane fabrication and testing. Does not look very complicated but since lots of different things can be tried I decided to estimate 3 weeks to achieve that.
- 9) **Extra time for the last details and imprevistos:** things I wanted to repeat or I did not have time to do. It is always nice to have extra time for stuff that might need to be improved or that was not done.
- 10) **Write the dissertation and prepare the presentation:** I wanted to write on the dissertation after reading papers, after finding the best parameter values and after all the device tests since the information was fresh and had fewer chances to forget things. I wanted to be sure I had enough time to do that.

Regarding the resources, I did not know what I was going to use since it mainly depended on how things evolved. However, the Nanoscribe printer, ovenplasma, ultrasonic bath, test tubes, IP-S resin, some chemicals and box samples, were going to be used. See Annex H for the list of materials and machines used.

At the end, the planning was pretty accurate in general. I had to start with the 3rd task, the nanoscribe induction a bit late because there were issues with my entry permit to the cleanroom, where the nanoscribe is. The 7th task, device test and improving geometry, was going on until the end so it was more a going back and forward process. I ended up printing for more than 3 weeks but I managed to do the things I was supposed to simultaneously so it had no effect on the rest of the tasks. The addition of pores and the membrane was done, instead, on the last two weeks of May. I wish I could have had more time for that task. However, it was enough to create a basic membrane and the pores. I spent two days seeing different procedures with mice that were going on in parallel projects: mice cancer induction, intellectual tests, etc. On the last week we implanted a device on the brain of a dead mouse to see how it would look like. The project was done under the supervision of Tobias E. Neagle a 3rd year PhD student at Cambridge University.

APPENDIX B. CODE

My project had no code development. However, DeScribe, the print job preparation software, created an autoscript that needed some adjustments to obtain the desired result (as commented in Chapter 5. Materials and Methods).

Since there is no program or code development this Annex will remain empty.

APPENDIX C. BUDGET

Here, I am including a summary of the budget in terms of the cost of the project realization. Taking into account the workforce and unitary costs of the materials and machinery that has been used.

CONCEPT	UNITARI COST	QUANTITY	TOTAL
WORKED HOURS	15£/h	570h	8 550£
NANOSCRIBE	60£/h	600h	36 000£
OBJECTIVE		1u	25 000£
CONSUMABLES			500£
		TOTAL	70 050 £

Table 7: Budget

I started working on the 1st of February on the project and ended on the 10th June. A total of 19 weeks and around 6 hours per day. Since I am working surrounded by PhD students I asked them how much they earned per month (2K£) and divided it for my monthly worked hours obtaining an average of 15£/h. It is not a very high wage but I guess that if you do research it is not for the money.

Regarding the Nanoscribe printings, the weekly average printing time was 40 hours (3 printing per week) and a total 15 weeks of printing which makes a total of 570hours.

The consumibles were chemical products (IP-S resin, acetone, isopropanol, PGMEA, among others), substrates, sample boxes, gloves, protection glasses and two coats for different uses (cleanroom and wetlab). That makes around 500£ spend on consumables. It is hard to calculate exactly how much I spent individually since different students used the same products and equipment sometimes simultaneously.

For the realization of this project, the department bought a 25K£ objective that has been added to the realization costs. The rest of the machinery has not been counted since it was already there.

The final cost of the project is 70 050£.

APPENDIX D. ETHICS COMMITTEE

For the development of my project any experimentation with people or personal data related to health were involved, as a result no ethics committee had to approve the project to guarantee the rights, safety or welfare of any participant.

However, devices were implanted into mice cadavers to verify the suitability for future animal experiments. The animals were used in an unrelated study and were culled according to schedule 1 UK 1886 animal scientific procedure act (ASPA). As no animals were culled specifically for the experiments in this thesis and the animals were not alive, no ethical approval or UK home office licence was required.

APPENDIX E. SLA PROCEDURE

1. The model under construction is positioned above the vat of photopolymer. The vat bottom is made from a flexible transparent Teflon film which is supported by a glass plate.
2. The model is moved downwards to one layer-thickness above the bottom of the vat. The movement squeezes photopolymer resin out from the gap between the model and the Teflon film. Viscous forces oppose the motion, resulting in mechanical deflection of the apparatus.
3. Four position encoders at each corner of the glass plate precisely monitor the mechanical deflection between the glass plate and the model under construction. The process monitors the deflection until it is relieved.
4. A cross-sectional image of the object being constructed is projected onto the underside of the vat film, causing photopolymer to harden in the shape of the image.
5. The model is lifted out of the vat to separate it from the vat film
6. The process is repeated until the model has finished building

The illustration of the process can be seen in Figure 51.

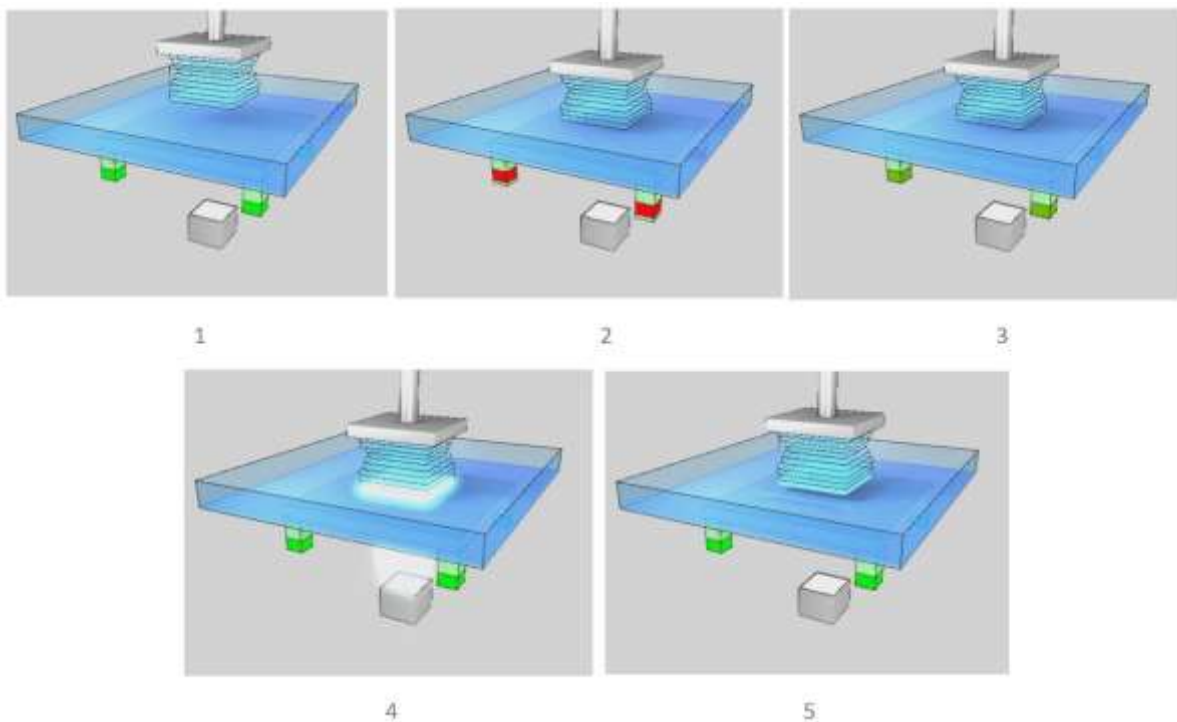


FIGURE 51: PRINTING PROCESS. SOURCE:

[HTTPS://WWW.WHIPMIX.COM/WP-CONTENT/UPLOADS/2021/06/MAX-USER-GUIDE-20190916.PDF](https://www.whipmix.com/wp-content/uploads/2021/06/MAX-USER-GUIDE-20190916.pdf)

APPENDIX F. PRINTING CONSIDERATIONS

F.1 NANOSCRIBE JOB RECIPE PARAMETERS

DEFAULT RECIPE: ('1P-S 25x ITO Balanced Swift (3D MF') **FINAL RECIPE:**

<p>Slicing.Mode = Fixed Slicing.DistanceMax = 1 Filling.Mode = Scaffold Filling.ShellContourCount = 5 Filling.BaseSliceCount = 2 Filling.ConcaveCornerMode = Sharp Filling.HatchingDistance = 0.5 Filling.HatchingAngle = 0 Filling.HatchingAngleOffset = 180 Scaffold.HatchingDistance = 1 Scaffold.Type = Planes Scaffold.WallSpacing = 20 Scaffold.FloorSpacing = 3 Scaffold.WallLineCount = 0 Scaffold.FloorSliceCount = 1 Scaffold.Offset = X:0 Y:0 Z:0 Scaffold.UseStagger = False Splitting.Mode = Rectangular Splitting.BlockSize = X:250 Y:250 Z:250 Splitting.BlockOffset = X:125 Y:125 Z:0 Splitting.BlockShearAngle = 20 Splitting.BlockOverlap = 1 Splitting.LayerOverlap = 2.5 Splitting.BlockOrderMode = Lexical Splitting.AvoidFlyingBlocks = True Splitting.GroupBlocks = True Splitting.UseBacklashCorrection = True Output.ScanMode = Galvo Output.ZAxis = Piezo Output.Exposure = Variable Output.InvertZAxis = True Output.WritingDirection = Up Output.HatchLineMode = Alternate Output.WritingOrder = ContourFirst Exposure.GalvoAcceleration = 10 Exposure.FindInterfaceAt = 2 Exposure.ShellLaserPower = 100 Exposure.ShellScanSpeed = 50000 Exposure.CoreLaserPower = 100 Exposure.CoreScanSpeed = 150000 Exposure.BaseLaserPower = 100 Exposure.BaseScanSpeed = 75000</p>	<p>Slicing.Mode = Fixed Slicing.DistanceMax = 1 Filling.Mode = Scaffold Filling.ShellContourCount = 5 Filling.BaseSliceCount = 2 Filling.ConcaveCornerMode = Sharp Filling.HatchingDistance = 0.5 Filling.HatchingAngle = 0 Filling.HatchingAngleOffset = 180 Scaffold.HatchingDistance = 1 Scaffold.Type = Planes Scaffold.WallSpacing = 20 Scaffold.FloorSpacing = 3 Scaffold.WallLineCount = 0 Scaffold.FloorSliceCount = 1 Scaffold.Offset = X:0 Y:0 Z:0 Scaffold.UseStagger = False Splitting.Mode = Rectangular Splitting.BlockSize = X:220 Y:220 Z:250 Splitting.BlockOffset = X:125 Y:125 Z:0 Splitting.BlockShearAngle = 20 Splitting.BlockOverlap = 20 Splitting.LayerOverlap = 20 Splitting.BlockOrderMode = Lexical Splitting.AvoidFlyingBlocks = True Splitting.GroupBlocks = True Splitting.UseBacklashCorrection = True Output.ScanMode = Galvo Output.ZAxis = Piezo Output.Exposure = Variable Output.InvertZAxis = True Output.WritingDirection = Up Output.HatchLineMode = Alternate Output.WritingOrder = ContourFirst Exposure.GalvoAcceleration = 10 Exposure.FindInterfaceAt = 0.6 Exposure.ShellLaserPower = 90 Exposure.ShellScanSpeed = 50000 Exposure.CoreLaserPower = 90 Exposure.CoreScanSpeed = 150000 Exposure.BaseLaserPower = 100 Exposure.BaseScanSpeed = 75000</p>
---	---

Table 8: Default vs current recipe.

The changed values are in bold. However, some of them were changed to be optimized but, by coincidence, were the same value as the default one, e.g. the shear angle). Other recipes could be as valid as this one, for instance the laser power value can be the same as the default one (100) or even lower values and still print an excellent device. However, sticking to this recipe guarantees a good printing for this prototype.

The main parameters that were helpful to achieve our (or any) structure are:

F.1.1 Writing parameters

PowerScaling: Sets the factor for the power scale on which LaserPower operates. PowerScaling 1.0 is the default setting for which LaserPower 0-100 operates between 0mW and the reference power at the objective aperture which is 50mW for the GT.

LaserPower: Sets the laser power in percent on the current power scale. ranges from 0-100%

ScanSpeed: Sets the writing velocity in $\mu\text{m/s}$. Increasing the ScanSpeed beyond that optimum will increase the writing time again. The position of that optimum depends strongly on the structure and the GalvoAcceleration.

GalvoAcceleration: This command controls the trade-off between writing time and structure quality in GalvoScanMode. Increasing this value reduces the writing time and increases the optimal ScanSpeed value but also reduces the writing quality most notably at the line starts and line ends. We recommend the parameter for this command to be between the default value of 1.0 and 20.0

F.1.2 Positioning commands

X/Y/Z Offset: Sets an offset for all programmed x/y/z-coordinates. The offset is added to each x/y/z-coordinate of each programmed or interpolated point. This command is useful to shift repeated structures in the writing area.

PiezoX/Y/ZOffset: Sets a piezo offset for all programmed x/y/z-coordinates. The offset is added to each x/y/z-coordinate of each programmed point.

MoveStageX/Y: Triggers a relative x-y-stage displacement on the x/y axis.

GotoX/Y: Positions the piezo or the x-y-stage to the defined x/y-coordinate, depending on the current ScanMode. For GalvoScanMode the positions will always be addressed with the piezo.

StageGotoX/Y: Positions the x-y-stage to the defined x/y-coordinate. This command ignores offsets and transformations.

AddZDrivePosition: Defines the movement of the z-drive of the microscope. It is absolutely necessary to use this command for structures higher than $300\mu\text{m}$ but it is also suitable for layer by layer writing.

F.1.3 Initialization parameters

SamplePosition: Moves to the defined sample position. The objective moves down, the x-y-stage addresses the defined sample center and an approach procedure is performed. This is different from double clicking on a sample position.

InvertZAxis: Triggers the inversion of the z-axis. To conserve a right-handed coordinate system, the x-axis is inverted at the same time. 0 deactivates InvertZAxis and 1 activates InvertZAxis

F.1.4 Protocol and logging

TimeStampOn: For TimeStampOn each message in the message log is marked with the current time

TimeStampOff: For TimeStampOff no time stamp is added to message log

DebugModeOn: Messages due to MessageOut and ShowVar will be displayed in the message log when loading structures

DebugModeOff: Messages due to MessageOut and ShowVar will not be displayed in the message log when loading structures

SaveMessages: Saves the current content of the message log in the file specified

ZDrivePosition: Writes the current position of the microscope z-drive to the message log

F.1.5 Batch processing parameters

Filling.HatchingDistance = Distance between hatch lines.

Scaffold.HatchingDistance = Distance between hatch lines for the scaffold.

Filling.SlicingDistance = Distance between slice lines.

Scaffold.SlicingDistance = Distance between slice lines for the scaffold (see Figure 52).

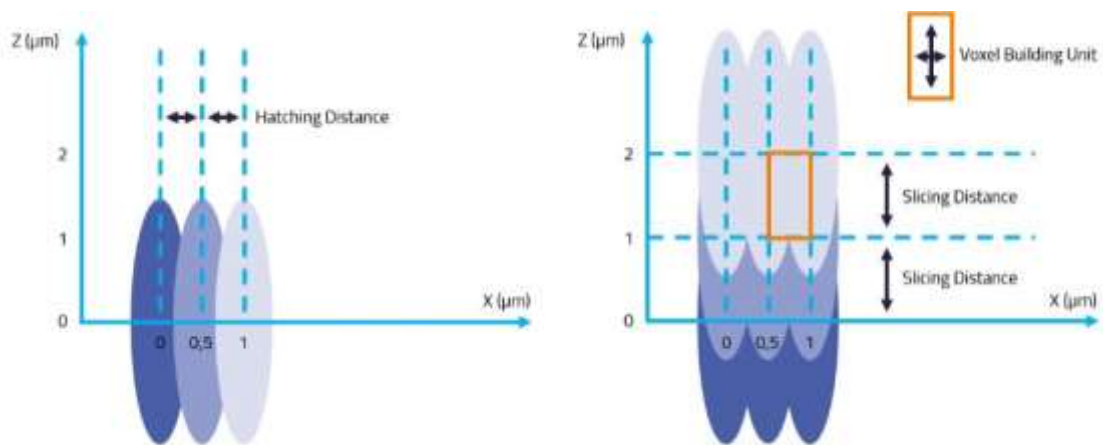


FIGURE 52: DEFINITION OF THE SLICING AND HATCHING DISTANCE THAT CREATES THE BUILDING BLOCKS FOR TWO-PHOTON POLYMERIZED STRUCTURES. SOURCE: [HTTPS://SUPPORT.NANOSCRIBE.COM/HC/EN-GB/ARTICLES/360000387254-ADVANCED-STL-PROCESSING](https://support.nanoscribe.com/hc/en-gb/articles/360000387254-Advanced-STL-Processing)

Scaffold.Type = Geometry of the scaffold: triangles, tetrahedrons, planes...

Splitting. Mode = The splitting of the structure into blocs: none, rectangular, hexagonal. Rectangular decreases blocks and printing time and hexagonal increases strength and printing time.

Splitting.BlockSize = X:220 Y:220 Z:250 The value is in [μm]

Splitting.BlockShearAngle = The definition can be better understood looking at Figure 50. However, if the angle is too small the shadowing effect results in poor stitching quality. Larger shear angles reduce the effective printing volume per block, increasing the print time. See Figure 53:

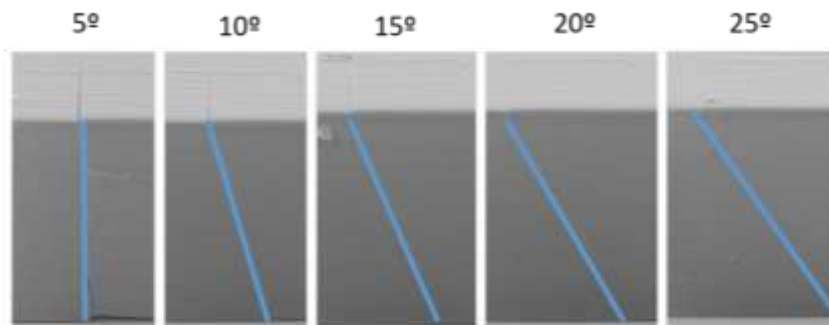


FIGURE 53: PRINTED CUBOID SPLIT INTO TWO BLOCKS WITH VARIOUS STITCHING ANGLES. THE SHADOWING EFFECT AT THE STITCH INTERFACE CAN BE OBSERVED AT LOW ANGLES.

Splitting.BlockOverlap = The block overlap of adjacent blocks (horizontal)

Splitting.LayerOverlap = The block overlap of adjacent blocks (vertical). See Figure 54:

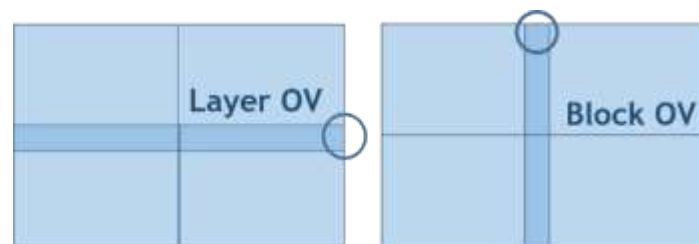


FIGURE 54: LAYER AND BLOCK OV

It is important that the BOV > hatching distance and the LOV > slicing distance otherwise there will not be verlap and stitching will fall.

Splitting.BlockOrderMode = The block printing order: lexical, meander, spiral. These determine the order in which the blocks are printed. Although meander and spiral modes decrease print time by minimizing stage movements, lexical block ordering results in smaller stitching errors.

Output.Exposure = Determines whether a single exposure setting (laser power and scan speed) is used for the whole structure or different settings for shell, core and base are applied.

Exposure.Shell(Core)LaserPower = The shell(scaffold) laser power; valid for both shell and scaffold set to constant [%].

Exposure.Shell(Core)ScanSpeed = The shell scan speed; valid for both shell and scaffold if Output.Exposure is set to constant [$\mu\text{m/s}$].

The laser power and scan speed at the objective lens can be adjusted to deliver a certain dose. The 3D Printer is calibrated to a certain mean power value (50mW) entering the aperture of the default objective, corresponding to a PowerScaling of 1.0 which is a factor from 0 to the maximum laser power the 3D Printer can deliver. The product PowerScaling x LaserPower determines the laser power at the lens, and LaserPower can range from 0-100%.

F.2 DEFAULT RECIPES FOR THE MF SOLUTION SET

- I. **Solid mode** for high precision, contour quality and shape accuracy.
- II. **Shell/scaffold mode** bypasses full-volume printing with inner support structures to increase print speed by a factor of 5 while maintaining the same high contour quality and shape accuracy.
- III. **Pure shell** is based on the shell/scaffold mode that stands for clean contours and thus increases printing speed by a factor of 7.
- IV. **Swift mode** is the sprinter among the DPP modes and prints about 10 times faster, in a quality that is impressive and is functionally adequate for many purposes.
- V. **Balanced swift mode** enables 6 times the speed with significantly improved precision.

Standard solid recipes are optimized for high precision at moderate throughput and offer the best structural stability. *Standard shell and scaffold* recipes are optimized for high surface quality and increased print speeds. Normally post-printing UV curing is required for improved stability. *Swift mode* recipes are optimized for maximal print speeds. If the application does not demand the highest surface quality, swift mode recipes could be appropriate. (UV curing is not required but can increase overall stability). See Figure 55 to see the visual differences between the different recipes.

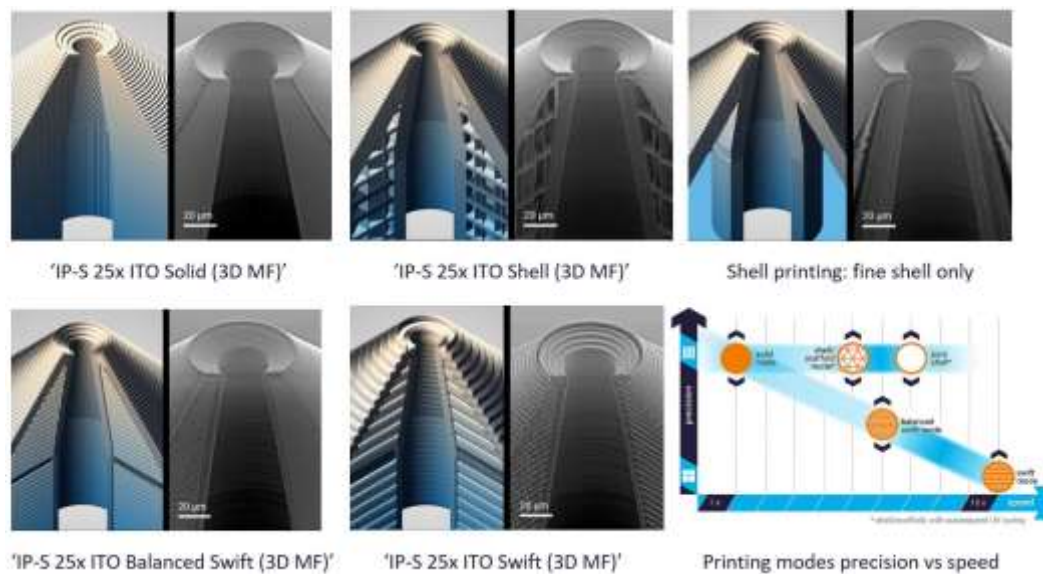


FIGURE 55: COMPARISON OF RECIPRE SOLUTIONS FOR THE 3D MF SOLUTION SET

'IP-S 25x ITO Solid (3D MF)' recipe printing: the entire volume of the object is sliced and hatched into fine parallel lines creating a homogeneous printed object. *'IP-S 25x ITO Shell (3D MF)' recipe printing*: Fine shell and triangular scaffold core. Requires post-print UV curing to polymerize the liquid core. *'Shell printing': fine shell only*. Requires post-print UV curing. The liquid core typically leads to bulging of the printed object during or after development. *'IP-S 25x ITO Balanced Swift (3D MF)' recipe printing*: fine shell and planar scaffold core. The surface roughness is comparable to the related shell recipe printing. The scaffold core consists of moderately connected planar slices. *'IP-S 25x ITO Swift (3D MF)' recipe printing*: coarse shell and planar scaffold core. The surface roughness is the coarsest of all printing modes. The scaffold core consists of weakly connected planar slices.

F.3 PRE-PRINTING CONSIDERATIONS

A script is generated automatically. To suit it to our prototype we added some lines and changed values (see Figure 56). The most important ones are:

- **DebugModeOn:** allows us to debug.
- **TimeStampOn:** in case the printing fails we can know exactly when.
- **ParameterMonitor:** allows us to see the parameters in the computer.
- **InvertAxis 1:** needed when the sample holder is inserted downwards; all glass substrates need that command whereas silicon does not need to be turned upside down because it uses oil immersion.
- **StageGoToX and StageGoToY:** allow us to move to print the structures in the substrate coordinates we want structures.
- **\$sweepDistanceX and \$sweepDistanceY:** minimum save distance between the printed structures, see Figure 50.
- **AddZDrivePosition:** allows us to move the objective up once the printing has finished to avoid crushing the objective with the structures.
- **SaveMessages:** everything that takes place during the printing gets written in a document.

```

lalala_sweep_job.gwl - Describe 2.6
File Edit 3D Preview Debug Window Help

lalala_sweep_job.gwl X
DebugModeOn
TimeStampOn
ParameterMonitor

! File generated by Describe 2.6

! System initialization
InsertZAxis 1

! Writing configuration
GalvoScanMode
ContinuousMode
PulseSettingTime 10
GalvoAcceleration 10
StageVelocity 200

! Scan field offsets
XOffset 0
YOffset 0
ZOffset 0

StageGoToX -7710
StageGoToY -7750

! -0500 450

! Writing parameters
PowerScaling 1.0

! Test parameters
TestScanSpeed 1000
TestLaserPower 40
TestPulseTime 15
LineSpacingY -30
TestPositionX -140
TestPositionY -250

! Sweep in X:
! ##### TESTS THAT WE ARE TRYING TO OPTIMIZE IN THE X AXIS

! Sweep in Y:
! Same as in Sweep X, for technical
! Exposure.CouplingPower System: 80 * 75 = 60

var $sweepDistanceX = 5000
var $sweepDistanceY = 5000

! DISTANCE BETWEEN 2 DEVICES --> formula to calculate the minimum

lalala_sweep_job.gwl - Describe 2.6
File Edit 3D Preview Debug Window Help

lalala_sweep_job.gwl X
MoveStageX 450.043 + $sweepDistanceX
MoveStageX 400 + $sweepDistanceX * -1

! Laser
MoveStageY -430.04345703125
LineNumber 4
LineDistance 100
FindInterFaceAt 0
writeText "X = 0, Y = 1500"
writeText "ShallLP = 700"
writeText "CoroLP = 90"
LineNumber 1
LineDistance 0
MoveStageY 430.04345703125

! Include slicer output
include lalalla_sub/lalalla_0_0_data.gwl

! DISTANCE !!!

! Custom writing parameters
set $contourLaserPower = 90
set $contourScanSpeed = 50 ! Only used when $contourPerfOrctStageMode = 0

! Solid body lines writing parameters
set $solidScanSpeed = 200 ! Only used when $solidPerfOrctStageMode = 0

MoveStageX 400 + $sweepDistanceX
MoveStageY 450.043

! Laser
MoveStageY -430.04345703125
LineNumber 4
LineDistance 100
FindInterFaceAt 0
writeText "X = 1, Y = 1500"
writeText "ShallLP = 900"
writeText "CoroLP = 90"
LineNumber 1
LineDistance 0
MoveStageY 430.04345703125

! Include v2Gcode output
include lalalla_sub/lalalla_0_0_data.gwl

AddZDrivePosition 2000
SaveMessages
  
```

FIGURE 56: SCRIPT GENERATED AUTOMATICALLY

Minimum Safe Distance Formula: $d = \frac{h-WD}{\tan \alpha} + \frac{D}{2}$, if we look at the table above we see that the $WD=380\mu\text{m}$, the $\alpha(\text{opening angle})= 31^\circ$ and the D (diameter at the top of the objective)= $5'2$. So in our case the formula will vary depending on the device height (h): $d = \frac{h-0.38}{0.6} + 2.6$. See Figure 57:

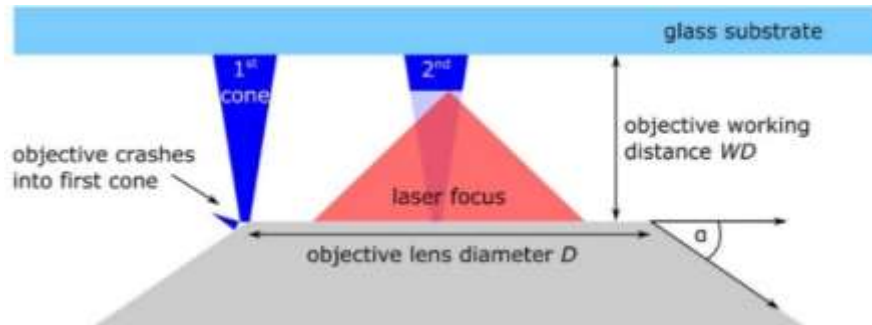


FIGURE 57: INFORMATION ABOUT THE REQUIRED PRINTING DISTANCE BETWEEN STRUCTURES THAT EXCEED THE WORKING DISTANCE OF THE OBJECTIVE. SOURCE: <https://support.nanoscribe.com/hc/en-gb/articles/360002482713-25x-OBJECTIVE>

We can pre-visualize the structure and its position in the substrate (that will help us avoid printing out of the substrate dimensions). Generate > Build 3D Preview > Bounding Box.

The Bounding box allows us to see how the structures will be placed without making the real shape of the device which would make the Generate 3D Preview much longer (see Figure 58).

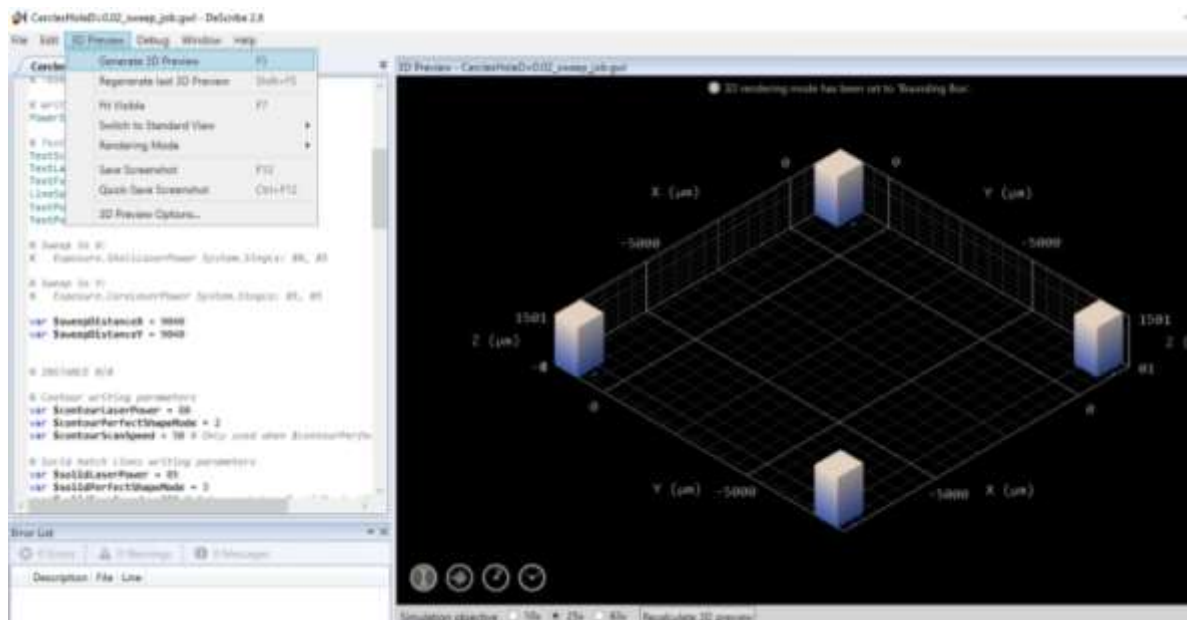


FIGURE 58: PREVISUALIZATION OF THE STRUCTURES

2PP systems typically have three scanning modes for photosensitive material polymerization as follows: (1) galvo, (2) piezo and (3) stage scan modes. The one we choosed in our recipe is the galvo since it is the faster and presents a good resolution as well. (We tried the others as well but there were no significant differences and the printing time for the others was almost doubled).

Scan mode	Laser beam	Photoresist (stage)	Uses
Galvo	Move in the xy directions	Remains stationary (z movement adjusted by the stage)	Larger structures (writing speed is faster)
Piezo	Remains fixed	Moved in xyz directions	High-resolution 3D structures (provides large travel range in 3 directions)
Stage Scan	Remains fixed	Moved in xyz directions	Larger areas but with lower resolution that the rest

Table 9: comparison between different scan modes

In contrast to conventional microfabrication, no spin coating, no photoresist thickness control, and no soft baking or post exposure baking of the photoresist are required; the fabricated structure simply has to be developed after photoresist crosslinking. Finally, the unexposed regions of negative-tone resist are removed in a developer bath. Additional flood exposure by UV light may be performed after development to trigger additional chemical crosslinking of the photoresists.

APPENDIX G. DETAILED PRINTING PROCEDURE

G.1 Sample preparation

The first step of sample preparation is substrate cleaning. After fixing the substrate to the sample holder, 2PP resins can be applied.

G.1.1 Substrate cleaning

The cleaning process consists of the following steps:

1. Rinse the substrate surfaces with acetone
2. Rinse the substrate surfaces with isopropanol
3. Rinse the substrate surfaces with distilled water (optional but recommended)
4. Blow-dry the substrate with nitrogen or air to remove residual moisture or solvent residues

Using this cleaning method, a droplet of 2PP resin will not spread out far over the substrate surface. Alternative cleaning methods or substrate preparation (e.g., oxygen plasma) change the wetting properties of the substrate surface. It might be a good solution when adhesion problems occur. It the beginning that is exactly what happened since we were still trying to find the good values of the parameters so often most of the structures just felt or were not solid enough) so we had to add an extra procedure, the oven plasma, also known as O₂ plasma cleaning. However, the adhesion could also be improved by silanization. Regarding the O₂ plasma cleaning, this is the process of removing all organic matter from the surface of an object through the use of an ionized gas called plasma. This takes place in a vacuum chamber using oxygen in an environmentally safe process (no harsh chemicals involved).

G.1.2 Substrate fixation and resin application

Substrates must be fixed securely and without large tilt angles on the appropriate sample holder using sticky tape (see Figure 53).

We choose the 9 square holes' base because we will be using a glass substrate with that shape (silicone substrates would work as well). Glass is cheaper but has less adhesion than silicone. However, glass has some recipes (which have proper default parameters) that are useful when printing, otherwise, it would take a longer time to print something decent. The center position (position five) which is the middle one offers the most uniform transmittance illumination and is preferably used when only one substrate is loaded. Because of these advantages, we choose the 9 holes' sample holder instead of the 3 holes and different shapes.

The ITO-coated substrates (3D MF DiLL) are the standard glass substrates for printing medium-sized features in DiLL in conjunction with the 25x objective. ITO refers to indium-tin-oxide.

When the substrate is placed in the base we proceed to check the ITO-coated side of the substrate which must face the objective. The 2PP resin must be applied to its conducting side because it

increases the refractive index contrast with respect to the 2PP resin. The ITO side can be identified with a simple multimeter, ohmmeter or diode polarity measuring device. We used the multimeter. The ITO-coated side must read a low resistance value of around 100-200 Ω . The glass side will measure “OL” meaning the resistance is too high to be measured. (see Figure 60).

We will secure the substrate with some sticky green tape. (or with the special screws but those aren't as strong as the tape; see Figure 59). When the deposition of the resin takes place we need to be sure that it is done in a constant pace and without moving the syringe too much in order not to create any bubbles).



FIGURE 59: SUBSTRATE FIXED ON (MULTI)-DILL SAMPLE HOLDER



FIGURE 60: ITO-COATED SIDE VS NO ITO-COATED SIDE

G.2 Sample loading, printing and sample unloading

We need to turn on the machine properly*. The loading process consists of the following steps:

1. Start and initialization of Nanowrite
2. Mounting an objective
3. Loading the sample holder
4. Sample approach
5. Loading a print job
6. Printing process
7. Unloading the sample holder

*there are some steps that must be followed carefully to keep the printer safe, for the full procedure check:

<https://support.nanoscribe.com/hc/en-gb/articles/360000733613-Powering-the-3D-Printer-Up-and-Down>

G.2.1 Start and initialization of Nanowrite

1. Open Nanoscribe Software.
2. Ensure that the microscope touchscreen displays: 'Lower z-limit reached' before starting NanoWrite. If this message is not displayed, manually and carefully lower the z-drive of the objective until it appears.
3. A Window will be opened automatically to calibrate the microscope; we will press Calibrate.
4. A sample holder and position can be selected.

G.2.2 Mounting an objective

It is really important for the pupil to never contact another surface. We are placing the 25x objective on its place (other resolutions are for other scales or purposes) we need to configure it as it is shown in Chapter 5. Insert it inside the nanoscribe and and:

- Place the felt ring to prevent 2PP resin creeping into the objective nosepiece.
- Check the correct objective is selected in the microscope screen (25x)

G.2.3 Loading the sample holder

Click Exchange Holder. That will centre the sample position first and lower the objective. Loading of the sample holder is now permitted. Ensure the sample holder is lined up the slider rails and insert with the label 'BOTTOM' pointing upwards. So we are turning it 180° to face the objective with the resin. Before inserting the base, we have to see 'z-lower reached' as a Pop up Message in the microscope screen and a 'choose base' window in the computer screen.

Once the sample holder is loaded, select the desired sample position and select the correct objective in the microscope screen and then press Approach Sample.

G.2.4 Loading a print job

- 1) Click Exchange Folder.
- 2) Turn the button Transmission On. See Figure 61.
(for the transparent substrates, reflection on for the opaque ones such as silicon).
- 3) Open AxioVision software.
- 4) Press the live button (AxioVision) and adjust the parameters to see a grey screen.
- 5) Load job (we load the filename_job.gwl file automatically generated by DeScribe).
- 6) Start Job.



FIGURE 61: TRANSMISSION BUTTON

G.2.5 Unloading the sample holder

When a print job is finished, click Exchange Holder. Then the stage will go to the center of the substrate but during this procedure the objective might drive into printed structures if the last structure is not the tallest or if it's as tall as the others. A solution is to issue an *AddZDrivePosition - 2000*, if Invert z-axis is disabled or 2000 if enabled. We already added that in the NanoWrite script Window.

G.3 Axiovision live-view camera settings

The printing process can be observed in the live-view window. Click Properties to open an image adjustment window with tabs that control the live-view image appearance. If we click BestFit in the Display tab is typically sufficient to display a well-balanced image (see Figure 62).

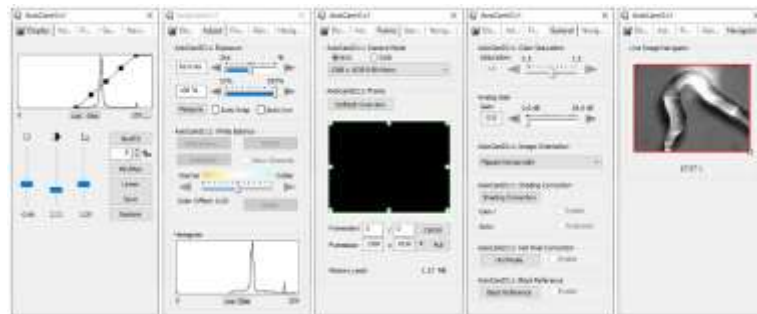


FIGURE 62: PROPERTIES WINDOW OF AXIOVISION. SOURCE: [HTTPS://SUPPORT.NANOSCRIBE.COM/HC/EN-GB/ARTICLES/360009720573-AXIOVISION-LIVE-VIEW-CAMERA-SETTINGS](https://support.nanoscribe.com/hc/en-gb/articles/360009720573-AxioVision-Live-View-Camera-Settings)

G.4 Post printing cleaning

Before we check the device we need to clean everything and close it properly

1. Take out objective and clean it with isopropanol carefully without touching the lens directly. Use lint free cloth or paper to tightly wrap around the objective. This material absorbs solvent during cleaning and prevents liquids from damaging the glue or internal optics. Hold the objective at a 45° angle and use a pipette to drop isopropanol onto the centre of the lens and absorbed by the paper or cloth. Repeat the process until residues are no longer visible (about 5-10 times).
2. Put the objective tap
3. Switch everything off (besides the big switch if we are printing in less than a week)
4. Clean everything with isopropanol (throw liquids inside the non-chlorinated waste bottle)
5. Put the sample inside a box sample and observe the results in the microscope

Cleaning steps have to be performed in a dust-free environment illuminated with yellow light. (The procedure took place in a 10K clean room with a yellow light room). Because white light may polymerize resin sitting on top of the objective lens and make cleaning and resin removal much more difficult or even lead to permanent damage.

APPENDIX H. MATERIALS AND MACHINES

H.1 Materials

The materials required in this project are given in the following list:

H.1.1 Nanoscribe printing

- ITO-coated glass substrates 3D MF DiLL 0.7mm thickness
- Sticky tape
- Nanoscribe sample holder and sample holder stand for an easier sample preparation
- IP-S resin
- 25x objective including felt ring
- Two 25mL beakers for sample development
- Beacker with tap (to prevent solvent evaporation during the development)
- Substrate holder (that fits into a 25mL beaker)
- Nitrogen gun for blow-drying
- Lens papers for cleaning optical surfaces
- Chemicals: PGMEA (mainly used as a developer for 3D-printed structuresagent and is suitable for cleaning spilles IP-S resin). Isopropanol (suitable for minor dirt such as finger prints, recommended for cleaning objective lenses), Deionized water (good starting solvent for cleaning many surfaces). Acetone (cleaning agent for substrates).

H.1.2 Others

- UV light source for post-print curing (SLA)
- GR-10 resin from Pro3dure
- Tweezers
- 33g Needles
- Norland optical adhesive 61
- Pipette
- 30cm of Fine Bore Polythene Tubing with an inner $d=0.4\text{mm}$ and an outer $d=0.8\text{mm}$
- Curing UV light
- 100Mm NaCl 5.84g/l
- 50ml/molar methanol blue
- UV-transparent cuvettes
- Fluigent lineup 340mbar pressure controller
- Sensirion 2145000155 (SLF3S-0600F) flow sensor

H.2 Machines

- Nanoscribe
- Asiga
- Emitech sputterer
- SEM
- Ovenplasma
- Ultrasonic bath
- Microscope
- UV curing oven
- Orbital shaker
- Magnetic hotplate stirrer
- Air extractor
- Computer with Autocad Inventor, DeScribe, Nanowrite and AxioVision software.